MONITORING OF THE DEGRADATION OF CHLORINATED ORGANIC IMPURITIES IN WATER BY AUTOMATED FLOW INJECTION ANALYSIS

by Amy Hong Que

B. Sc., Jilin University, 1984

M. Sc., Jilin University, 1987

A THESIS SUBMITTED IN PARTIAL FULFILLMENT OF

THE REQUIREMENTS FOR THE DEGREE OF

MASTER OF SCIENCE

in

THE FACULTY OF GRADUATE STUDIES

DEPARTMENT OF CHEMISTRY

We accept this as conforming

to the required standard

THE UNIVERSITY OF BRITISH COLUMBIA

March 1994

© Amy Hong Que, 1994

In presenting this thesis in partial fulfilment of the requirements for an advanced degree at the University of British Columbia, I agree that the Library shall make it freely available for reference and study. I further agree that permission for extensive copying of this thesis for scholarly purposes may be granted by the head of my department or by his or her representatives. It is understood that copying or publication of this thesis for financial gain shall not be allowed without my written permission.

Department of _CHEMISTRY_

The University of British Columbia
Vancouver, Canada

Date _MAY 10, 1994_

DE-6 (2/88)

ABSTRACT

Chlorinated organics are a major concern because of their persistence in the environment, possible toxicity and carcinogenicity. One of the substances of most concern, chloroform, has been classified as a priority pollutant by U.S. Environmental Protection Agency. It is present at trace levels in man-made drinking water and in waste water from industries such as pulp and paper. The scope of this thesis has been to develop instrumentation and methods for destruction and detection of chloroform and related contaminants in such samples.

Attack of chloroform by free radicals (*e.g.*, HO·) can result in complete mineralization: *i.e.*, quantitative liberation of the innocuous free chloride and generation of carbon dioxide. Free radicals are formed when a suspension of a semiconductor material such as titanium dioxide is illuminated with ultraviolet light. They are also formed when aqueous solutions are subjected to a high intensity ultrasonic field. In this thesis we report use of both UV and ultrasound to degrade chloroform, and have monitored the rate and extent of conversion via real-time on-line measurement of free chloride concentration and conductivity. The technique used for these studies is Flow Injection Analysis.

Specific objectives of this research were as follows:

(i) To develop a photo-reactor within which to carry out the degradation experiments. This contained two mercury lamps and used either suspended titanium dioxide powder (anatase) or titania glass as photocatalyst. The two UV lamps were directly immersed in the solution to provide the most efficient UV irradiation. A 23 kHz sonicator probe was situated in the centre of the vessel for those experiments which required it.

(ii) To develop an automated sampling system by which the progress of the reaction within the reactor could be followed. This was comprised of polytetrafluoroethylene (Teflon®) tubing and contained an in-line microfiltering system to

remove catalyst solids. It was used to take samples from the reactor and deliver them to the detection system.

(iii) To develop an automated Flow Injection Analysis system to detect products from the photodegradation of the organic species. A flow-through conductivity detector was constructed and used to monitor the change in total free ions. A chloride ion selective electrode with its flow-through cell was used to quantitatively monitor the change in concentration of free chloride ion. In both cases the output was observed as a series of skewed Gaussian peaks.

(iv) To characterize the instrumentation developed and to use it to study the degradation of chlorinated organics - specifically chloroform. The instrumentation was able to monitor the progress of reactions over a period of several hours without human supervision. With the presence of UV light and titania powder catalyst it was found that chloroform was totally degraded after about 50 min. The chlorine was quantitatively recovered as chloride ions. A kinetic analysis showed that the reaction curve followed $A \rightarrow B \rightarrow C$ reactions. A mechanism for the reaction is proposed in the thesis. When using a heterogeneous chloroform system, introduction of power ultrasound into the reactor improved the yield after 20 min by 41 % based on the detection of chloride ions. A preliminary investigation of a glassy form of titanium dioxide showed a reaction rate which was four times slower than for the anatase form, given equal masses. This rate difference may be due to decreased contacting surface area. However, the glassy form is much easier to use.

The system developed has strong potential for rapid, semi-automatic development of optimal catalytic treatments to detoxify industrial waste water and purify municipal drinking water. As such it has significant economic and environmental applications.

TABLE OF CONTENTS

LIST OF FIGURES

LIST OF SCHEMES

LIST OF TABLES

ACKNOWLEDGMENTS

CHAPTER 1

INTRODUCTION

Chlorinated organics are a major concern to the environment. One problem with some of these chlorinated organics, and the reason why they are termed persistent, is that it can take decades or even centuries for them to break down naturally. Because of this persistence and their high solubility in fat, they tend to accumulate in the tissues of some animals (a process called bioaccumulation). The contamination is then passed through the food chain and can reach very high concentrations in the tissues of predators [1].

Chlorinated organics enter ecosystems by many pathways, including industrial discharges and leakage, municipal and consumer wastes, and run-off from agricultural and forestry applications. They are used as insecticides, such as DDT (*di*chloro*di*phenyl*tri*chloroethane), and in various industrial applications, such as PCBs (polychlorinated biphenyls). Other important sources are the by-products of certain chlorination processes. Chlorination is widely used to disinfect waste water, drinking water [2] and swimming pools. Industrial uses of chlorine include bleaching of wood pulp [3]. Water chlorination does more than eliminate unwanted color and destroy bacteria; chemical reactions take place between chlorine and organic materials present in water to form chlorinated organics. Some of the chloro-organic compounds formed exhibit acute and chronic toxicity to aquatic organisms. Chloroform, for example, is toxic and carcinogenic. It is a common synthetic product arising at ppb (parts per billion) levels during municipal chlorination of drinking water supplies [4-7]. Although it is not an acute hazard to humans at the levels detected (the minimum lethal dose (MLD) of chloroform to a human being is 15 ml /70 kg person [8]), its presence suggests the need to monitor and

1

to determine whether there may be a chronic long-term threat to the populace. The U.S. Environmental Protection Agency (US EPA) has classified chloroform as a "priority pollutant" [9] and has set a recommended maximum concentration of 100 µg/l in drinking water [10].

One possible mechanism for the formation of chloroform can be deduced from the compounds detected in tap water. Trihalogenated methanes and ethanol were found in tap water but mono- and dihalogenated compounds could not be detected [6]. Ethanol oxidizes to acetaldehyde, which in turn, reacts with free chlorine to form chloral. Water combines with chloral to form chloral hydrate, which then decomposes to form chloroform. The reaction scheme is:

$$CH_3CH_2OH \longrightarrow CH_3CHO \xrightarrow{Cl_2} Cl_3CCHO \text{ (chloral)}$$

$$\xrightarrow{H_2O} Cl_3CCH(OH)_2 \longrightarrow CHCl_3$$
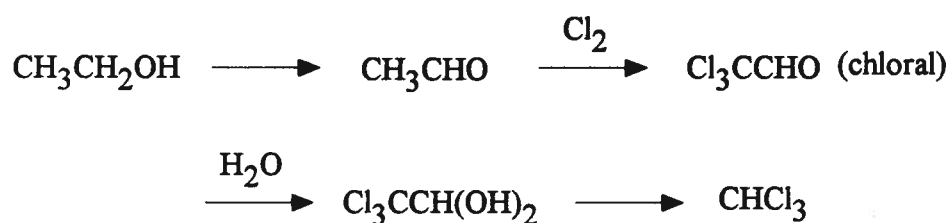
Using chlorine to bleach pulp results in the formation and subsequent discharge of chlorinated organic matter. Chloroform is one of the most abundant volatile chlorinated compounds found in effluent from the C-stage (Chlorine) of bleaching of wood pulp [3, 11-13]. This stage has been identified as the major source of chloroform release to the atmosphere [13]. Therefore, chloroform has been of significant interest to the pulp and paper industry in British Columbia and elsewhere. The industry is switching more of its production to chlorine dioxide bleaching, which results in far less chlorinated material in the waste stream (effluent).

1.1 DEGRADATION OF CHLORINATED ORGANICS IN WATER

Concern over chloroform and other chloro-organic compounds in the aqueous environment has prompted research into methods for their degradation. Catalyst-assisted photodegradation, biodegradation, chemical degradation and ultrasonic degradation are some of the more common methods.

Ideally, a water treatment process for degradation of trace halocarbon contaminants should yield innocuous products such as carbon dioxide, hydrochloric acid and water. This is referred to as "complete mineralization". Since toxicity of chlorinated aliphatic hydrocarbons decreases with chlorine content [14], partial degradation with dehalogenation may result in partial detoxification. Hydroxylation of carbon-chlorine bonds (with release of free chloride) is usually the important step in the degradation and is particularly effective at detoxification. In part this is because the addition of a hydroxyl group into the molecule makes the compound more polar and hence more soluble in water, and makes the substance biologically more reactive [15]. From another perspective, the resulting products from hydroxylation tend to be excreted more readily by living organisms. The following sections will briefly describe degradation methods which have been commonly investigated.

1.1.1 PHOTODEGRADATION USING TITANIUM DIOXIDE

Recently, a method for destroying organic impurities has attracted much attention because of its possible use in purifying drinking water and waste water. This method is based on the powerful catalytic ability of the semiconductor titanium dioxide (anatase form) when exposed to near-ultraviolet (UV) light. It is fast and does not necessarily require addition of liquid reagents. Titanium dioxide is activated only by photons of wavelength $\lambda \leq 350$ nm [16]. Heterogeneous photo-assisted catalysis has been shown to be an effective method for complete mineralization (to dissolved CO_2 and HCl) of dilute

3

aqueous solutions of many common chlorinated organic compounds [17]. Complete decomposition of aliphatic polychlorinated compounds, such as chloroform ($CHCl_3$) [16,18], dichloromethane (CH_2Cl_2) [16], carbon tetrachloride (CCl_4) [16] and trichloroethylene (Cl_2CCHCl) [14] has been reported. Rate parameters for degradation of these polychlorinated compounds have been obtained by Ollis [19]. Most aromatic compounds and chlorine substituted aromatics are more intractable than aliphatics. Complete mineralization requires cleavage of the aromatic rings. Titanium dioxide suspensions illuminated with UV light have been used for this purpose [17]. According to Barbeni *et al*, aqueous solutions of 4-chlorophenol (4-CP) [20] and pentachlorophenol (PCP) [21] are almost completely decomposed to CO_2 and HCl. Kinetics of such reactions have been actively studied by Matthews [17, 22] and Ollis [19].

Mechanism

In the presence of oxygen, several *n*-type semiconductor powders have been shown to behave as photo-catalysts and promote the oxidation of substances. Powders of semiconductors such as TiO_2 offer many advantages for desorptive decomposition. Toxic compounds can be readily adsorbed to their surface, which can then be activated through UV irradiation or attachment of reactive species. Irradiation of a semiconductor such as TiO_2 with light of energy higher than the band-gap results in creation of positive holes (h^+) in the valence band and electrons (e^-) in the conduction band of the semiconductor [23]. These charge carriers can recombine without further reaction. Alternatively, the holes can be scavenged by oxidizable species (for example H_2O, H_2O_2, or a hydrocarbon RH), and the electrons by reducible species (for example, O_2 or H^+) in the solution. Scheme 1.1 shows the reactions which occur [23].

4

$$TiO_2 \xrightarrow{\text{\textit{hv}}} TiO_2{}^* \;(h^+ + e^-)$$

$$H_2O \;+\; h^+ \;\rightarrow\; HO\cdot \;+\; H^+$$

$$HO^- \;+\; h^+ \;\rightarrow\; HO\cdot$$

$$H^+ \;+\; e^- \;\rightarrow\; H\cdot$$

$$O_2 \;+\; e^- \;\rightarrow\; O_2{}^{\cdot-} \xrightarrow{H^+} HO_2\cdot$$

$$2HO_2\cdot \rightarrow O_2 + H_2O_2 \xrightarrow{O_2{}^{\cdot-}} HO\cdot + HO^- + O_2$$
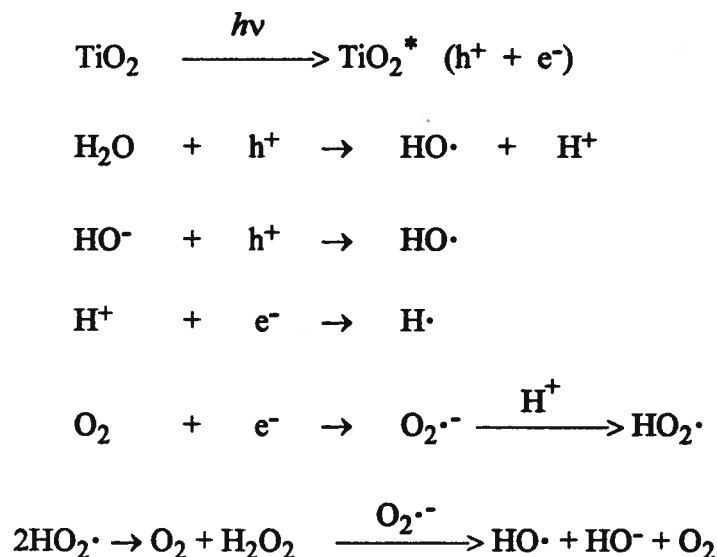
Scheme 1.1 Proposed mechanism of production of HO· radicals

The hydroxyl radical, HO·, produced as an intermediate, plays an important role in the oxidation process. It is an indiscriminate, electrophilic, highly reactive species which degrades organic components of any water system. The hydroxyl radical is more reactive than its parent and is responsible for the major pathway to the hydroxylation of organics. Organics may be quantitatively oxidized, stepwise, by such reactions — eventually to CO_2 and HCl.

Tokumaru and coworkers [24] have demonstrated that hydroxyl radical, HO· is formed via the oxidation of water by a positive hole (h^+) of TiO_2 with concurrent removal of the electron by molecular oxygen. Bard *et al* [25] demonstrated the formation of HO· radical on TiO_2 photocatalyst under illumination by using spin-trapping. The probable role of HO· in oxidation reactions is also supported by the reaction of Fenton's reagent with benzoic acid [26] and chlorophenols [27]. Fenton's reagent is a mixture of hydrogen peroxide and a reducing agent such as ferrous ion which gives hydroxyl radicals, HO·.

$$Fe^{2+} + H_2O_2 \;\rightarrow\; Fe^{3+} + HO\cdot + OH^-$$

The hydroxyl radicals produced oxidize benzoic acid and chlorophenols completely to carbon dioxide, hydrochloric acid and water.

The mechanism of decomposition of chlorinated hydrocarbons is summarized as follows: in aqueous solution, the surface of TiO_2 is covered with OH^- as well as H_2O. These species may react with the photo-generated hole (h^+) to produce $HO\cdot$. Chlorinated organics in aqueous media are adsorbed onto the surface of the catalyst. The carbon-chlorine bond may then be attacked and chlorine substituted by the electrophilic species $(HO\cdot)$ to form an alcohol. The alcohol may be oxidized by photo-generated holes and highly reactive, reducible hydroxyl radicals to form aldehydes or ketones. These are easily oxidized further to carboxylic acids. Carboxylic acids can be decomposed to CO_2 via the "photo-kolbe" reaction [26, 28, 29]. Chlorine radicals are converted to chloride ions by capture of electrons. The presence of molecular oxygen and water are essential to this reaction scheme [14, 20, 21].

If the intensity of the light is sufficiently high, the photocatalytic powders cannot absorb all of the incident photons. Thus, this radiation can cause homogeneous photolysis reactions, in addition to the desired heterogeneous photocatalytic degradation processes. This renders detailed mechanistic studies of such systems very difficult.

The effect of molecular oxygen on photodecomposition

Molecular oxygen is required stoichiometrically for complete mineralization of organic impurities. For example,

$$CHCl_3 + H_2O + 1/2\ O_2 \xrightarrow{\quad TiO_2/h\nu \quad} CO_2 + 3\ HCl$$
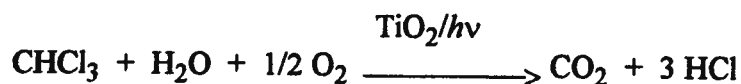
Molecular oxygen acts as an electron acceptor to scavenge the photo-generated electrons during formation of HO· via oxidation of water by the photo-generated holes. This serves as a competition reaction for the recombination of photo-generated holes and electrons.

$$H_2O \quad + \quad h^+ \quad \rightarrow \quad HO\cdot \quad + \quad H^+$$

$$O_2 \quad + \quad e^- \quad \rightarrow \quad [O_2^-]_{TiO2}$$

$$[O_2^-]_{TiO2} \quad + \quad e^- \quad \rightarrow \quad [O_2^{2-}]_{TiO2}$$
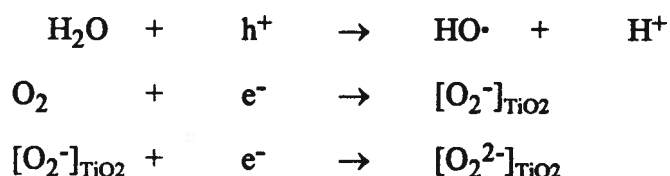
Hydroxyl radicals and peroxides are important intermediates involved in the decomposition process because they are powerful oxidizing agents. The fact that some organics degrade slowly or are incompletely degraded could be due to the amount of hydroxyl radicals and peroxo groups generated on the surface being a limiting factor.

Molecular oxygen is a very convenient oxidizing agent for most photocatalytic oxidations since it is readily available in air. Oxygen may enter into solution by several routes: (1) from fresh liquid, (2) by exposure of powder-containing solution to air, (3) through the walls of the reaction vessel which may be porous to oxygen, and (4) by deliberate aeration of the solution.

1.1.2 SONOLYSIS WITH POWER ULTRASOUND

Ultrasonic oxidation has been reported as a method of degrading toxic materials such as phenols and chlorophenols in waste water in general, and in bleach plant effluent in particular [30]. When an aqueous medium containing organic halogen compounds such as CH_2Cl_2, $CHCl_3$ or CCl_4, is irradiated with ultrasound, the carbon-halogen bond is cleaved [31]. Sonication of solutions results in localized extreme reaction conditions. Cavitation bubbles form and collapse. The localized pressures and temperatures generated are

sufficient to cause rupture of the O-H bond of water with the formation of hydroxyl radicals and hydrogen peroxide [31, 32]. Ultrasound irradiation also increases the activity of powder catalysts [33] since it causes remarkable changes in particle aggregation, surface morphology and (for powdered metal catalysts) thickness of oxide coatings. It is increasingly used to initiate and promote chemical reactions [31, 32, 34]. Turai [35] reported that ultrasound improved the biological activity of bacteria used in waste water treatment by increasing the availability of oxygen and mass transfer of the pollutants to and from the bacteria.

The sound spectrum

The normal frequency range of human hearing is between 16 Hz and 16 kHz. Ultrasound is defined as the sound having higher frequency than that to which the human ear can respond. It is generally considered to lie between 20 kHz and 500 MHz (Figure 1.1) [36].
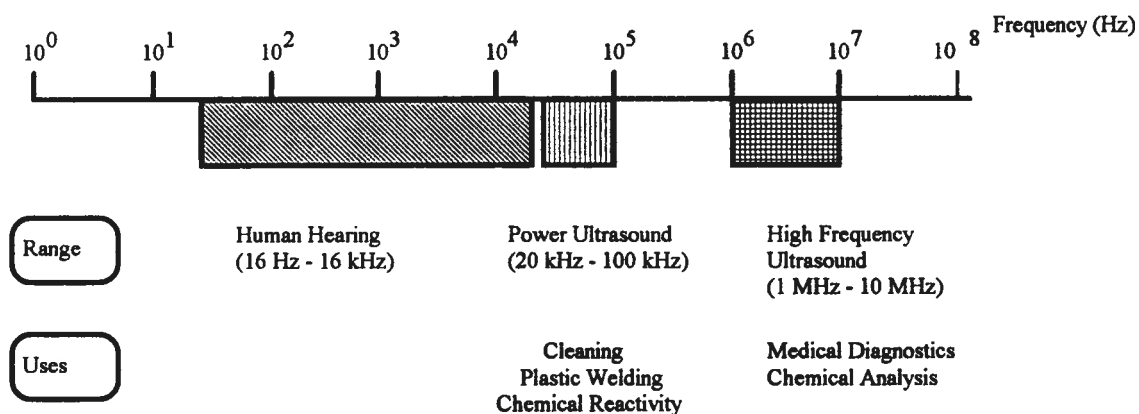
Figure 1.1 Sound frequencies

The use of ultrasound within this large frequency range may be divided into two principle areas: (1) power ultrasound and (2) high frequency ultrasound. Power ultrasound involves relatively higher power and low frequency waves between 20 kHz and 100 kHz. Applications include cleaning, plastic wielding, and more recently to affect chemical reactivity. High frequency ultrasound involves high frequency, low amplitude propagation. It is used in medical scanning, chemical analysis and studies on relaxation phenomena.

Ultrasound production

For economic reasons mainly, 20-50 kHz is the region most commonly used. The required power and frequency range useful for chemical purposes is generally produced by an ultrasonic transducer or converter which converts either mechanical or electrical energy into high frequency sound. Commonly used transducers which produce power ultrasound are piezoelectric crystals and magnetostrictive devices. The operation of the former is now described.

A piezoelectric crystal, such as quartz, is coupled to suitable electrodes, and when an alternating current of ultrasonic frequency is applied, the crystal vibrates (expands and contracts) producing ultrasound. The transducer crystal vibrates in the longitudinal direction and transmits this motion to a microtip (Figure 1.2). The material used for the tip should have high dynamic fatigue strength, low acoustic loss, be resistant to cavitation erosion and be chemically inert. The best material by far is titanium alloy.
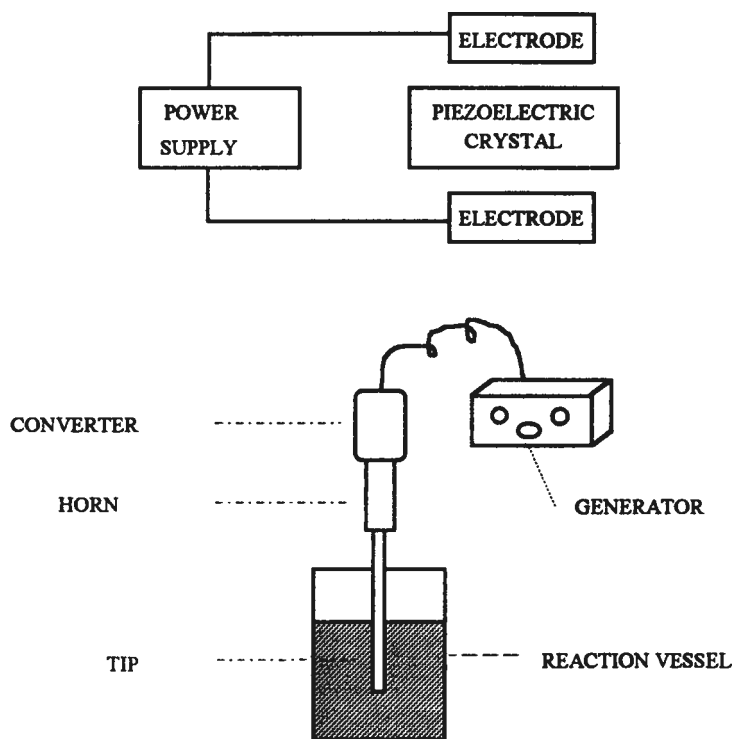
Figure 1.2 Schematic diagram of an ultrasonic probe system

Chemical effects of power ultrasound

Most chemists who have an interest in sonochemistry concentrate on power ultrasound, since this type of sound provides sufficient energy to affect chemical reactivity [31].

The physical phenomenon caused by power ultrasound which is responsible for most of the chemical effects is *cavitation* [34]. Like any sound wave, ultrasound is transmitted as a pressure wave through a medium. During each "stretching" phase a fluid medium can literally be torn apart, provided that the negative pressure is strong enough to overcome intermolecular binding forces. Cavitation produces tiny micro-bubbles (cavities) of approximately 100 nm in diameter. In succeeding compression expansion cycles, these cavities grow until they become unstable, whereupon they collapse violently

10

in less than a microsecond with the release of large amounts of energy in the immediate vicinity of the micro-bubbles. The likelihood of cavitation occurring increases with aeration and power applied, and decreases at high frequencies (> 50 kHz) [36].

It has been estimated that transient local temperatures of up to several thousand Kelvin (> 5000 K) [37] and local pressures of up to one hundred atmospheres are produced during this collapse. In the immediate vicinity of the imploding bubble the powerful shock wave produced on collapse will create a jet at roughly 400 km/h through the solution [34]. It is the violent implosion of unstable cavities which generates these momentarily extreme local temperatures, pressures and shock waves, and which provides a unique environment for chemical reactions.

1.1.3 OTHER POSSIBLE METHODS

Chemical oxidations by ClO_2, H_2O_2 and Fenton's reagent ($H_2O_2 + Fe^{2+}$) [38] have also been studied for the purpose of disinfecting and bleaching. High chemical demand, the consequent high cost, and the chemical contaminants introduced externally can preclude the use of such chemical degradation as a viable treatment alternative in some circumstances. Nevertheless, ClO_2 has replaced (or partially replaced) Cl_2 bleaching in many kraft mills.

The metabolism of chlorinated molecules by bacteria can also contribute to environmental detoxification. Two reports have dealt with the aerobic biodegradation of pentachlorophenol (PCP) [39, 40]. Hydrocarbons are now known to be biodegraded by numerous environmental microorganisms. However, many halogenated compounds are biodegraded poorly and the most highly halogenated molecules appear to be metabolized exceeding slowly.

Other possible approaches to disinfect drinking water [41] and ground water [42] include ozonation and irradiation by ultraviolet light. Ozone is now being used instead of

11

free chlorine in production of bleached kraft pulp [43]. Ozone, short-lived in water, is an extremely strong disinfectant, second only to fluorine. It is also a chlorine-free disinfectant and may one day lead to complete elimination of man-made chlorinated substances from effluents. Two types of ozone reactions occur in natural waters: direct ozonation reactions and free radical ozonation reactions [41]. Direct ozonation reactions, which involve the ozone molecule, are highly selective and relatively slow. The free radical ozonation reactions involve the autocatalytic decomposition of ozone, which results in the production of the same highly reactive but unstable intermediate mentioned previously - the hydroxyl radical. This free radical has been observed to be a less selective and more powerful oxidant than ozone itself.

Ozonation has its own problems. Ozone reacts selectively with organic compounds and usually cannot decompose the organics completely to carbon dioxide and water [44]. Also ozone is very unstable, with a half-life of just 15 minutes at room temperature. This means it must be produced on-site, using processes which require high consumption of electrical energy.

High temperature processes such as incineration [45] may be used satisfactorily to treat waste hydrocarbon liquids or vapors which contain difficult chlorinated components. However, such high temperature treatments of very dilute halocarbon aqueous solutions are economically impractical.

1.2   REAL-TIME REACTION MONITORING BY FIA

Real-time monitoring of the reactions described above requires either *in-situ* sensors (within the reaction vessel) or analytical systems which sample the contents of a reaction vessel at regular intervals, and track the concentrations of key species present. Flow injection analysis (FIA) has been proven to be a suitable methodology. It is an ideal tool for liquid sample handing, pretreatment of samples prior to their determination, and selective detection of analytes. Separation techniques such as in-line filtration can be implemented and provide reproducible results. FIA systems provide fast, precise, and accurate analyses. They are simple to operate and straightforward to automate; the latter property results in decreased labor expenses. The small volumes of solution required per analysis minimize reagent volumes used, sample costs and waste disposal problems. An automated FIA system provides a means of carrying out an analysis in a closed system, thus materials which are toxic or unstable in air may be more conveniently and safely analyzed than by a manual method.

1.2.1   PRINCIPLES OF FLOW INJECTION ANALYSIS (FIA)

Principles of flow injection analysis and function of a flow system

Flow injection analysis is based on injection of a liquid sample into a moving, non-segmented continuous carrier stream of a suitable liquid. The injected sample forms a zone, which is then transported towards a detector that continuously records the absorbance, electrode potential, or some other physical parameter(s) of the stream as it continuously changes due to the passage of the sample through the detector flow cell [46, 47].

A simple flow injection analyzer (Figure 1.3) consists of a pump, which is used to propel the carrier/reagent stream through a narrow tube; an injection port, which

introduces a well-defined volume of sample solution into the carrier stream in a reproducible manner; a reaction coil in which the sample zone disperses and possibly reacts with the components of the carrier stream; a flow-through detector which quantitatively detects the chemical species of interest; and a recording device [46]. FIA is based on the combination of three principles: sample injection, controlled dispersion of the injected sample zone, and reproducible timing of its movement from the injection point towards and through the detector.
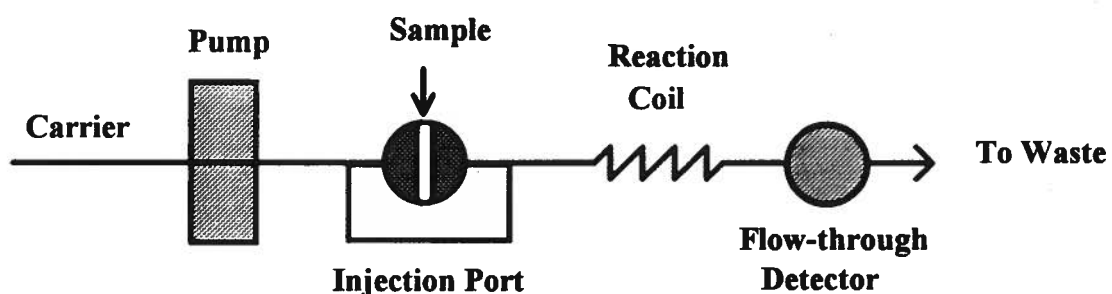
Figure 1.3 Single-line FIA manifold

A well-designed FIA system has an extremely rapid response: the residence time t_r, which is the time between the injection and the peak maximum is in the range of 5-20 s. The residence time also defines the period for chemical reaction, if any. A sampling cycle is typically less than 30 s. The injected sample volumes are usually between 10 and 250 μl. Thus, FIA is a simple, microchemical analytical technique, capable of having a high sampling rate (~120 cycles/h), minimal sample and reagent consumption, and can produce results in near real-time.

Dispersion of the sample zone

A sample solution contained within the injection valve prior to injection is homogeneous and has original concentration C^o. If it could be scanned by a detector, a square signal would be produced, the height of which would be proportional to the sample concentration (Figure 1.4, left). When the sample zone is injected, it follows the movement of the carrier stream and forms a dispersed zone whose shape depends on the geometry of the channel, the flow velocity, time of sample residence in tube, viscosity and the diffusion coefficient of analyte solution [48]. Hence a concentration gradient is formed and the peak-shaped response curve reflects a continuum of analyte concentrations and dispersion (D) values (Figure 1.4, right).
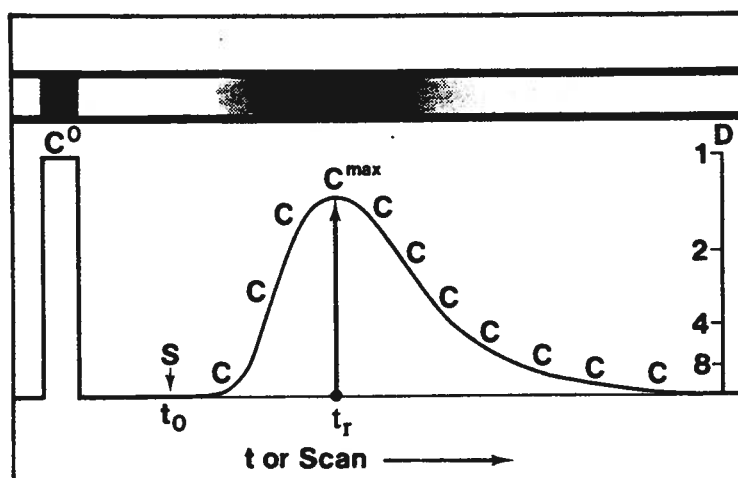
Figure 1.4 Schematic representation of the effect of dispersion on an injected sample zone.

Transport conduit cross-section - top;   Concentration profile - bottom
        No dispersion - left;   Dispersion - right

Two physical processes, convection and diffusion, are responsible for sample dispersion. The former is induced by flow and causes the sample zone to acquire a parabolic head and tail; the latter causes the concentration profile across the zone to take

15

on a Gaussian shape. Combination of convection and diffusion results in FIA peaks typically being described as skewed Gaussian peaks.

In FIA, excessive dispersion results in loss of sensitivity. Sufficient dispersion is required for mixing and reaction to take place and (usually) for the production of a concentration gradient. In order to design an FIA system rationally, the dispersion coefficient D has been defined as the ratio of concentration of sample material before and after the dispersion process has taken place [49]:

$$D = C^o / C$$

where D is the dispersion coefficient, C^o is the original sample concentration and C is the concentration after dispersion. This is shown on the right hand side axis of Figure 1.4.

FIA Readout

When recorded, the transient signal observed by a detector during the passage of the dispersed sample zone has the form of a peak. The height H, width W, or area A of a peak is related to the concentration of the analyte present (Figure 1.5) [46].
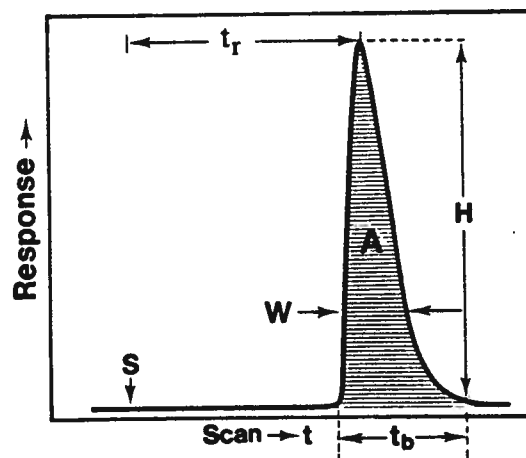
Figure 1.5 A typical recorder output

H: the peak height   W: the peak width at a selected level
A: the peak area t_b: the peak width at the baseline
t_r: the residence time   S: injection of sample

16

Peak height, H, is the most frequently measured peak dimension in FIA since it is easily identified and directly related to detector response, such as absorbance, potential, current, *etc.* Provided that the detector used responds linearly to the concentration of the sensed species, then peak height is a linear function of analyte concentration:

$$H = a + bC$$

where a and b are intercept and slope constants. Peak height is most commonly measured at peak maximum, but (especially for high concentrated samples) may also be measured at any other point along the response curve.

Peak area, A, is similarly to peak height, directly related to the detector output. It can provide improved sensitivity over peak height since it involves integration over a larger number of data points. However, its use is somewhat restricted by the difficulty in eliminating baseline noise and determining accurately the beginning and end of the peak. Furthermore, it cannot be used as accurately for "log(C) detectors" such as ion selective electrodes: It distorts the readouts, since that portion of response which is close to the baseline disproportionally weighs much more than the portions of readout close to the peak apex.

Peak width, W, typically measured as full width at half maximum of the peak (FWHM), is logarithmically dependent on analyte concentration. It has a wider dynamic range than peak height and peak area measurement, but is less precise. Peak width measurements have been used in specialized applications such as titrations.

1.2.2 PROCESS MONITORING BY FIA

FIA is finding increasing applications in chemical routine analysis and research, teaching of analytical chemistry and monitoring of chemical processes. Perhaps the fastest growing area of interest is in using FIA for process control. The main reason is that by

analyzing the chemical composition of process streams in near real-time the process operation can be tuned to its optimal level [50]. Optimization is of great importance for economic reasons, since it allows better use of raw materials and energy. Other advantages of the results of optimization include corrosion prevention, environmental protection, prevention of the production of undesirable, toxic or otherwise hazardous by-products, compliance with stringent statutory regulations; and ensuring high product quality and product quality reproducibility.

Advantages of use of FIA in process control

Most sensors developed for detection of chemical components cannot be installed directly in the process stream, since they can quickly suffer from erosion, occlusion, poisoning or other physical damage. Also, regular calibration of some *in-situ* on-line process sensors is very difficult. In process control applications, flow injection analyzers automatically take, pretreat, and analyze samples. Their control microprocessors then the data and communicate results with the process environment. They offer many practical benefits which enhance the attractiveness and acceptance of on-line chemical analysis as part of closed-loop control.

(1) They facilitate near real-time continuous monitoring by regularly aspirating sample solution (for example, from a batch-type chemical reactor) into a carrier solution, the detector being operated in an impulse response mode. Thus a chemically modulated signal, continuously recorded as a series of peaks, offers a valuable measurement of both the detector and process performance. Near real-time measurement is an important objective to be pursued in process analysis.

(2) One important advantage of using a pulsed technique in process control is the constant check on baseline drift (Figure 1.6) [51]. In continuous FIA, a nearly complete return to the baseline can be achieved between two successive injections by a proper selection of the injection frequency. In this way, it is easy to correct for slow fluctuations

of the background. Detector fouling can be prevented by means of a periodic wash sequence, perhaps using dilute acid and/or a detergent. Occasional injections of standard solutions allow further control of detector performance, thus ensuring that the magnitude of the recorded peaks truly reflects the concentration of the monitored species (and not deterioration of the response characteristics of the detector).
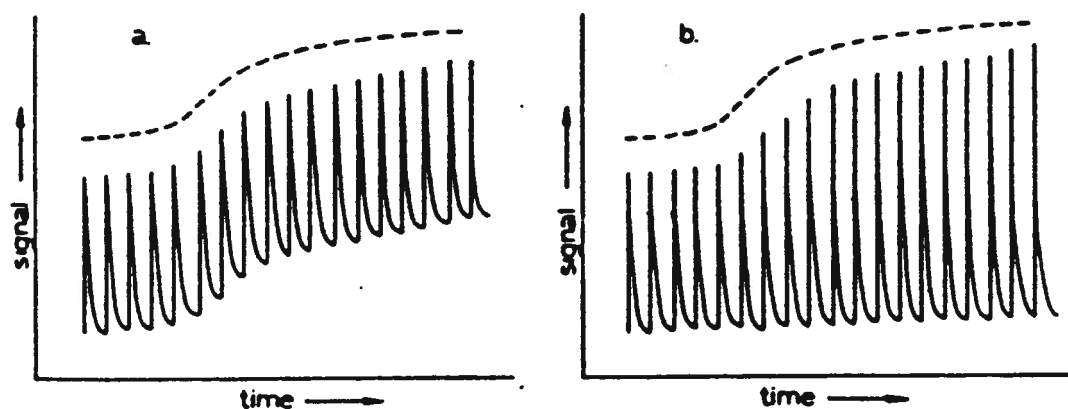
Figure 1.6 Analyzer response *vs.* time.

(a) No concentration change; drift of baseline.

(b) Concentration change; constant baseline.

Key: (—) Flow injection device; (---) Continuous monitoring device.

(3)   The profile of the transient signal obtained with plug injection can provide a trained operator with valuable information about the correct functioning of any flow injection system.

(4)   The operation costs of FIA are low because of low consumption of reagent and sample. The operation and maintenance of FIA systems are generally simple.

FIA approaches for process control

There are three approaches for process control applications utilizing peak height as the source of information. They are based on sample injection, standard injection and reagent injection.

Sample injection (Figure 1.7) follows the scheme most frequently used in laboratory applications of FIA: a solution from a reactor, or a stream to be monitored, is (after possible pretreatment) propelled by a pump (P1) into an injection valve, which, when turned, injects the analyte into the carrier stream, merging downstream with a suitable reagent. After passage through a reaction coil, within which the species to be monitored is produced, the sample zone enters the detector, which continuously records the composition of the stream. A sufficient amount of time is allowed to transpire between individual injections, so that baseline is re-established, indicating that the system has been thoroughly washed and that the detector is functioning properly. Calibration can be performed before, after, or even during the monitoring period by injecting standard solutions. Computer control of the FIA system allows for precise timing of events (injection, start-go pumping sequences, data collection, and recalibration).

Standard injection involves continuously pumping and monitoring analyte solution. An occasional injection of a standard allows periodical control of the response of the system. The drawback of the standard injection approach is that the FIA channel and the detector are not periodically washed by a cleansing carrier solution and might therefore become contaminated.

Reagent injection saves reagent(s) consumption by injection of small amount of reagents only at the times when a readout is required, while the analyte solution is pumped continuously through the FIA channel. Since detectable species are formed only in the presence of the reagent(s), the readout still has the form of a peak. A series of peaks is obtained that reflects the change of analyte concentrations during the monitoring period. Calibration is achieved by aspirating standard solutions instead of sample solution.
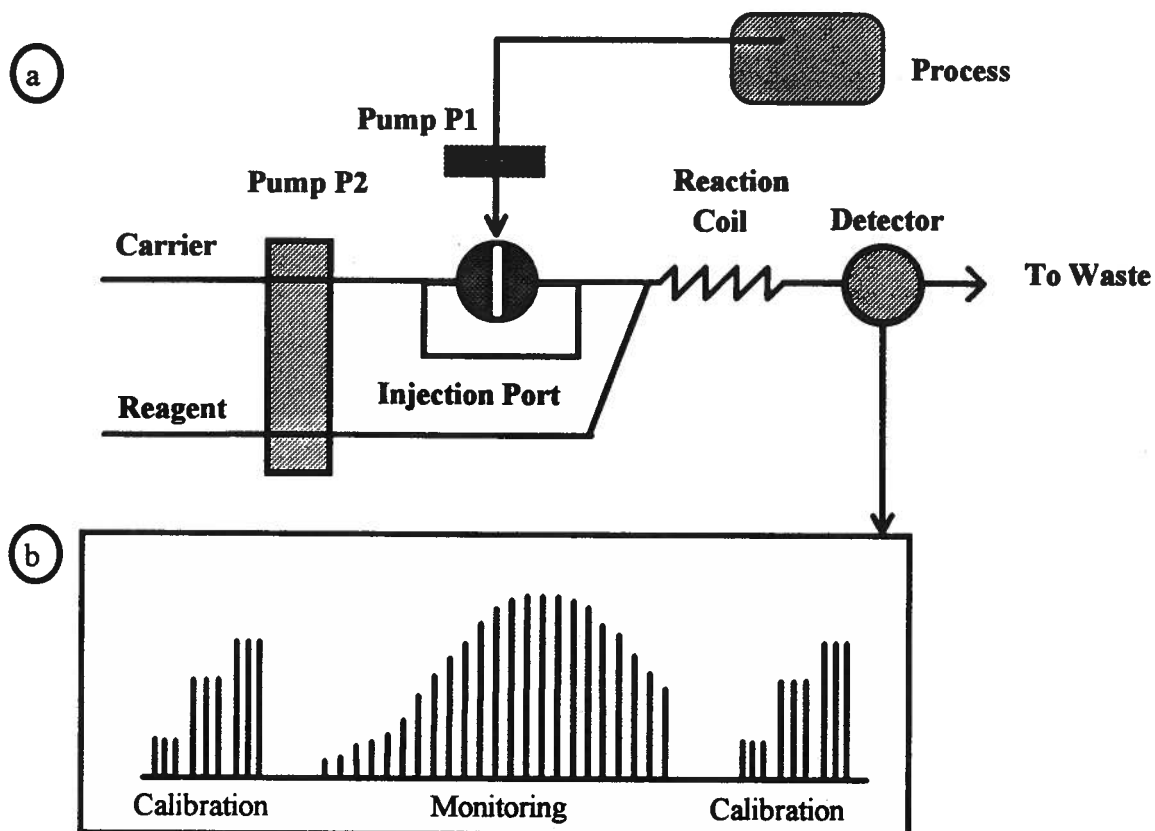
Figure 1.7 Continuous monitoring based on sample injection

(a) The sample, aspirated from a process reactor by pump P1 is intermittently injected by a valve into the carrier stream which is merged with reagent solution, propelled by pump P2. (b) Before monitoring the process, the system is calibrated by injecting a series of standards. This procedure is repeated after the monitoring period. The baseline is reached between each injection, thereby allowing control of the performance of the analyzer itself.

Flow injection analyzers have been used for in-process surveillance of caustic streams [52], hydroperoxide [53, 54] and analysis of commercial bleach [54]. Chemical production [55-59], biological waste water treatment [60], and biotechnological processes [61-65] have been reported to be controlled by FIA techniques. Ruzicka [66], Van der Linden [51] and Gisin *et al* [67] summarized the advantages of using FIA for industrial on-line process control and detailed a number of FIA approaches and techniques for process monitoring.

1.3 MONITORING DEGRADATION OF CHLORINATED ORGANICS BY FIA

Environmental contaminants present in an aqueous suspension of titanium dioxide powder (anatase) can be degraded with UV light [21, 22, 68-72]. According to Zeltner, this technology has not as yet been successfully commercialized [73]. Difficulties remain in separating the titania (anatase form) particles from the suspension after degradation has occurred and in finding a simple, low cost, low labor consuming method to monitor the degradation process.

One solution to the separation problem is to immobilize the titanium dioxide powder on a support that is transparent to UV irradiation. This kind of photo-reactor with immobilized TiO_2 on an inner support surface is usually wrapped on or set parallel to UV lamps, and is compatible with flow based monitoring systems. Most of the glass photoreactors studied employ Pyrex glass as the support [73]. Pyrex was chosen because it is much less expensive than quartz and much easier to fabricate. In addition, titania coatings adhere very well to Pyrex, but such coatings readily delaminate from hardened silica or quartz. However, Pyrex is only transparent to UV radiation down to a wavelength of about 340 nm and absorbs most of the radiation of wavelength $\lambda < 300$ nm

[73]. Titanium dioxide is activated only by photons of wavelength ≤ 350 nm [16]. Quartz is transparent to all UV wavelengths [19].

Use of such a reactor in the flow injection determination of organic solutes in water was first reported by Low and Matthews [74]. The reactor was constructed by first immobilizing a thin film of titanium dioxide onto the inner surface of a length of Teflon tubing then wrapping the treated tubing around a near-UV illuminating source - a "black light" tube. The advantage of attaching the titanium dioxide to a stationary support is that the solution for oxidation may be passed continuously over the illuminated photocatalyst en route to some detector. Hence, the process can be monitored in real-time. The in-line reactor was installed after the injector port of the flow system. An organic compound (methanol) injected in the flow stream was oxidized photocatalytically to carbon dioxide, which was subsequently monitored by a conductivity detector.

Another solution to the problem of separating the TiO_2 catalyst is to filter out the titania powder prior to the determination. Barbeni [21] reported off-line centrifugation and filtration through a 0.22 μm Millipore filter to remove the suspended solids. Ollis [14, 16, 18] designed a recirculating, differential conversion photoreactor in which "black lights" (UV lamps) were oriented parallel to the reactor axis. An aqueous slurry of titanium dioxide was recirculated with a pump, centrifuged and monitored potentiometrically by a chloride ion selective detector in the line. This required a large amount of solution. The detector was easily contaminated, in which case, performance rapidly deteriorated.

1.4   OBJECTIVES

The main objectives of this thesis were to develop a photocatalytic degradation method for destroying chlorinated organics and to develop a automated FIA instrumentation for the real-time monitoring of the degradation process.

The specific goals were as follows:

(1)   To develop a photo-reactor within which photocatalytic degradation reactions could occur. The photo-reactor would contain a vessel to hold the solution, UV lamps to illuminate UV irradiation, photo-catalysts and a sonicator to produced power ultrasound when needed.

(2)   To develop an in-line sampling system within which the solution would be sampled and pretreated prior to the detectors.

(3)   To develop an in-line automated FIA instrument to monitor the degradation process in real-time. This would contain a pump to propel the carrier solution, a injection valve to inject the pretreated sample, and the proper flow-through detectors to monitor the products and/or reactants.

The developed system would be used to examine the priority pollutants such as chloroform ($CHCl_3$) using aqueous suspensions of titanium dioxide illuminated with UV light in a batch reactor. The photodegradation process would be monitored by an automated flow injection analysis system by regularly aspirating sample solutions from the photo-reactor. The samples would be filtered prior to injection into the flow injection system. A process monitoring curve would be produced.

In this work, four different strategies were evaluated: UV irradiation alone, UV irradiation with TiO_2 catalyst (anatase), ultrasound irradiation alone, and their combination. It was also considered important to investigate other solutions to the problem associated with using TiO_2 powder. One of our objectives was to explore the

24

catalytic ability of another form of TiO_2 -- a TiO_2 glass. With this, there is no separation procedure needed for the system because titania glasses are large pieces of glass and tend to reside at the base of the solution, unlike the titania powder which is suspended throughout the solution. No paper has yet reported use of titania glass as a catalyst to photodecompose aqueous organic impurities.

It was hoped that this work, automatically monitoring the degradation of chlorinated organics using FIA, would lead to improved fundamental knowledge of the degradation kinetics and mechanism for chloroform.

CHAPTER 2

INSTRUMENTATION

2.1 DEVELOPMENT OF PHOTO-REACTOR FOR PHOTODEGRADATION OF AQUEOUS CHLORINATED ORGANICS

2.1.1 REAGENTS

Chloroform was analytical reagent grade (BDH Inc., Toronto, Ontario). Milli-Q water, obtained from a Milli-Q purification system (Chemistry Department, UBC), was used for all solutions and had a specific resistance greater than 18 MΩ cm. Anatase TiO_2 was obtained from Tioxide, UK, with a surface area of 10.8 m^2/g, as determined by BET[1] * nitrogen adsorption. Glassy TiO_2 was obtained from Dr. H. D. Gesser, Chemistry Department, University of Manitoba, with a determined BET surface area of 91.6 m^2/g.

2.1.2 APPARATUS

Preliminary Studies

A flow-through reactor similar to that of Low and Matthews [74] was initially built. They immobilized a thin film of titanium dioxide onto the inner surface of Teflon tubing then wrapped it around a 20W "black light". The "black light" emitted ultraviolet light of between 320 nm and 400 nm. In this work we used silicone or Teflon tubing wrapped around a 100W mercury UV lamp which gives its most intense light at 254 nm.

---

[1]* BET (Brunauer, Emmett and Teller) nitrogen adsorption method is used for the determination of surface area of the solids. The method assumes that the volume of nitrogen gas adsorbed by the solid in the frozen system is equal to the volume of nitrogen gas released when heated, for a given mass of solid. The theory is based on the ideal adsorption isotherms. It assumes: (1) a single molecular layer of adsorbed species and that (2) the energy of adsorption is invariant.

Responses were observed from both the conductivity detector and chloride ion selective electrode when Milli-Q water was passed through the tubing. As the time of UV irradiation increased, the signal from both detectors increased. The silicone and Teflon tubing had been washed sequentially with 1% (w/w) nitric acid and purified water to remove any contamination. Any possibility of a temperature effect caused from the UV lamp was eliminated by insertion of a cooling bath prior to the detectors. The effect was attributed to tubing etching resulting from the mercury lamp, which had higher energy and higher power than the "black light" tube. Because of these difficulties this design was not pursued in our study, and a more conventional reactor design was employed.

Photoreactor

Figure 2.1 shows the photo-reactor cell then designed for degrading chlorinated organic compounds. The reactor vessel was a 250 ml pyrex beaker situated in a water bath which was maintained at room temperature. Anatase TiO_2 photocatalyst (typically 0.05 wt%), used in most of the experiments, was added to the reactor. Then aqueous solutions (200.0 ml) containing various concentrations of chloroform [typically ppm (mg/l) level] were placed in the reactor. UV-light was provided by two mercury vapor lamps (Model 80-1127-01, BHK Analamp, CA.) and a power supply (Model 90-0001-01, BHK Analamp, CA.). The lamps were quartz-jacketed and rated as ozone free. They emitted light at wavelengths from 185 nm to over 600 nm with the most intense wavelength at 254 nm. Each lamp had a length of 12.7 cm and an outside diameter of 0.9 cm. They were directly immersed in the sample solution to a depth of 10 cm. The system provided the most efficient irradiation to organic pollutants in aqueous solution because no medium which absorbed UV light existed between the solution and the UV source.
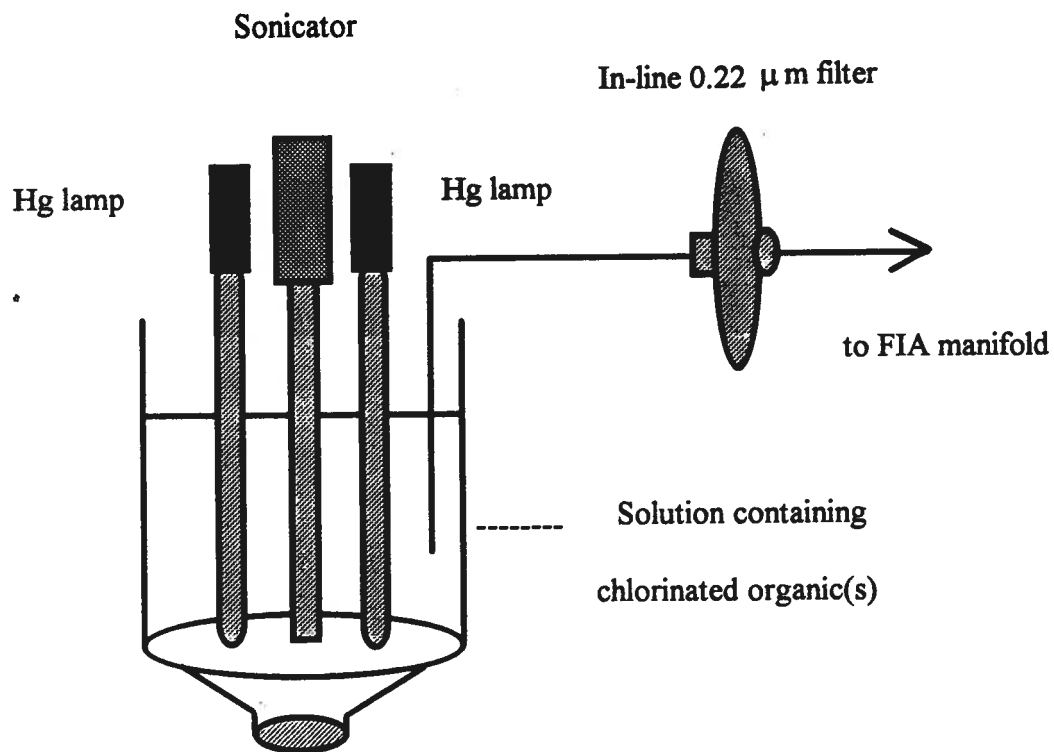
Figure 2.1 Reactor for sono/photolytic degradation of chlorinated organics in water.

(The solution may contain TiO_2 suspension.

The entire reaction vessel is situated in a water bath.)

The solubility of chloroform in water at room temperature and 1 atm total pressure is 8.2×10^3 mg/l. Chloroform, which has a specific gravity of 1.49 g/ml, is heavier than water. At concentrations above or close its solubility in water, chloroform is immisible with water and collects at the base of the reactor as a separate organic phase. An outwardly protruding dimple (1 cm deep, 1 cm in diameter) was made at the bottom of the beaker to hold that drop of chloroform for experiments which used for a high concentration of chloroform and power ultrasound. The dimple holds that drop of chloroform so that power ultrasound can be effectively directed at it.

The power ultrasound probe was immersed into the solution when it was needed. The reactor was open to expose the TiO_2 mixture solution to the atmosphere so that oxygen from air could be used for degradation. The suspended solution was stirred by a magnetic stirrer during the entire degradation process. To protect the operator from UV irradiation, the whole reactor was covered with aluminum foil (obtained locally).

Sonicator

In our system ultrasound was generated by a sonicator probe (Microson Model XL2005, Heat Systems - Ultrasonics Inc., Farmingdale, NY) which is a reliable 23 kHz source designed to economically supply over 50 watts average output into very low volumes (250 μl to 40ml or more). The unit used a titanium microtip (3 mm dia.). The tip was immersed directly into the solution until the end was about 2.5 cm from the base of the vessel. This provided the most efficient radiation to the chloroform layer. The most intense sound is produced at the tip of the probe and intensity decreased with distance from the tip.

Sampling System

A peristaltic pump (Model C6V, Alitea USA, Medina, WA) was used to propel the carrier stream (Milli-Q water). A microfilter, which consisted of two plastic shells (25 mm dia.) sandwiching a 0.22 μm pore-size membrane (MSI, Cat. No. 64534, Westboro, MA), was situated in the sampling line to filter out particulate TiO_2 catalyst (anatase). Polytetrafluoroethylene tubing (Teflon®, 0.8 mm i.d.) was used throughout. The sample solution undergoing UV irradiation (and possibly sonication) was aspirated by a sampling pump through the micro-filter and propelled to the injection loop of the FIA system. Aluminum foil was wrapped around the tubing in the sampling line to keep UV from illuminating the tubing: ions were found to be released from Teflon tubing under UV irradiation.

2.2 DEVELOPMENT OF AUTOMATED FIA MANIFOLD FOR MONITORING THE DEGRADATION OF CHLOROFORM

The FIA manifold developed for monitoring the degradation of aqueous chloroform is shown in Figure 2.2. It was constructed from components available within this laboratory. Sample solutions and carrier were propelled by two separate peristaltic pumps. Samples were injected using a six-port, air-driven, solenoid-actuated injection valve (Type 5020P, Rheodyne Inc., Cotati, CA) and control circuitry designed in this laboratory. The chloride ion selective electrode was a combination chloride electrode (Model 96-17B, Orion, MA). The conductivity detector was built in our laboratory. All components were controlled by a microcomputer via a data acquisition and control adapter (described later). Operating software, also written in this laboratory, was available to control and/or monitor pumps, injection valve and detectors. It was written in Microsoft Quickbasic version 4.00 and is discussed elsewhere [75, 76, 77].
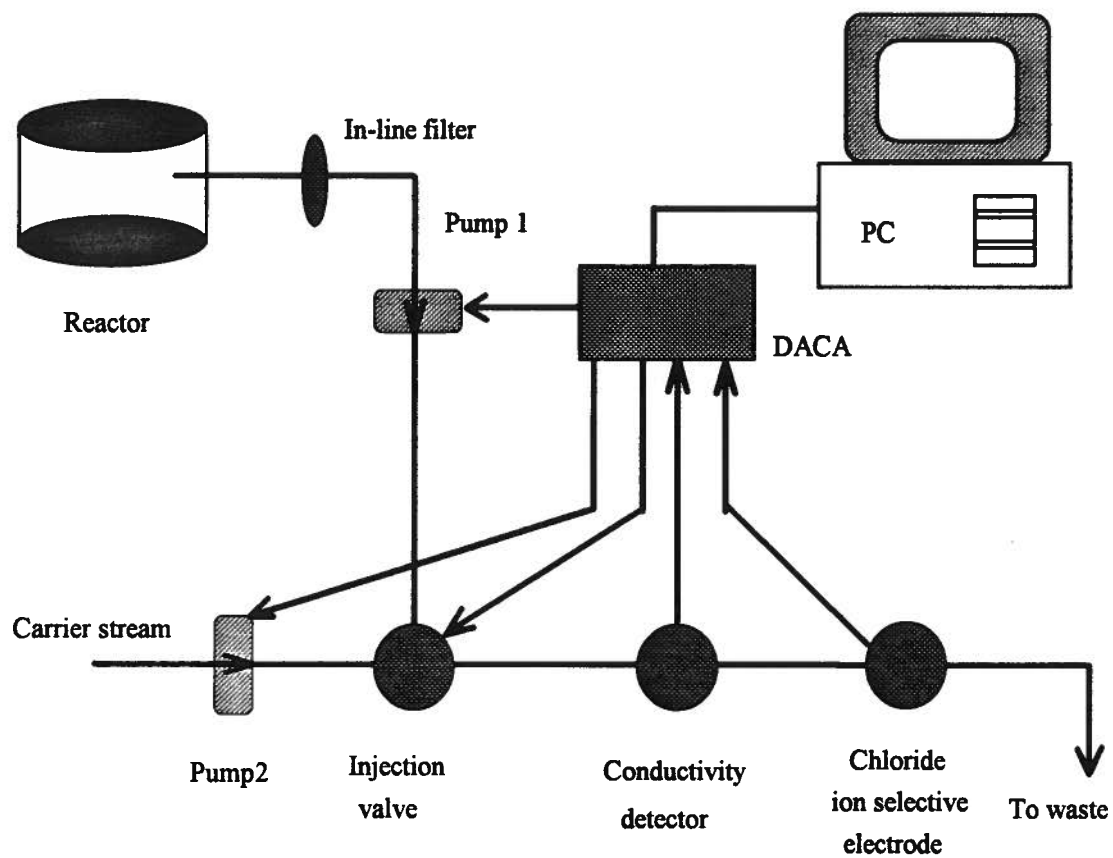
30

Figure 2.2 Monitoring the degradation of chloroform by flow injection analysis

Samples which had undergone UV irradiation (and/or sonication) were first propelled by a pump through an in-line microfilter to remove any catalyst powder. They were then injected by an injection valve into the carrier stream (Milli-Q water) which was propelled by another pump so that they were transported through a chloride ion selective electrode and a conductivity detector. The two pump speeds were set at 0.79 ml/min and were calibrated gravimetrically. The distance between the two detectors was 3.0 cm. In this way, free chloride ions and total free ions produced from the degradation were monitored by both detectors simultaneously, rapidly and automatically. The whole process which included sampling, filtration, sample injection, analyte detection and data collection was automated with a microcomputer.

The best performance of FIA systems is obtained when peak broadening effects are kept to a minimum. These arise from manifold geometry, flow velocity, the hold up volume of the detector flow-through cell, the speed of detector response, and the time constant of the associated electronics. All these factors were considered in its design.

This system provides real-time continuous monitoring capability by regularly aspirating sample solution from the reactor into the carrier stream. Signals were recorded as a series of peaks. Calibration was performed before and after the monitoring period to obtain quantitative measurements of chloride ions produced. Peak heights reach a flat plateau, indicating the process has come to the end.

2.3   COMPONENTS OF FIA SYSTEM

2.3.1   COMPUTER FOR CONTROL AND DATA ACQUISITION

Control of the flow injection development and optimization system was accomplished with an IBM-PC compatible computer (Nora Systems, Vancouver, B.C.) which issued commands to and/or monitored responses from all hardware components.

The computer communicated with the FIA system via an IBM data acquisition and control adapter (DACA) board (Mendelson Electronics, Dayton, OH).

The IBM DACA board has 16 digital input and output lines, four channels of 12-bit analog-to-digital (A/D) conversion and two channels of 12-bit digital-to-analog (D/A) conversion. The first eight digital output lines (BO0-BO7) are used to provide data to the external interface which is addressed with the next three lines (BO8-BO10). These three address lines allow up to eight external independently addressable devices to be used. Digital outputs BO11-BO14 are used to provide direction control for the two Alitea pumps. Digital inputs BI0 to BI16 are used to return status information from external devices.

The four analog-to-digital converter (ADC) inputs can, in most cases with instrumentation constructed in this laboratory, be connected directly to detector outputs. Differential inputs are used and the voltage range is usually set at -5V to +5V. Alternative ranges of 0V to +10V and -10V to +10V are switch selectable on the DACA board. The two digital-to-analog converter (DAC) outputs are used to control the speed of the Alitea pumps and set to an output range of 0 to +10V.

2.3.2 PUMPS AND TUBING

Solutions were propelled via two peristaltic pumps (Model C6V, Alitea USA, Medina, WA). They are capable, in principle, of maintaining a constant volumetric flow rate. The main drawback of peristaltic pumps is pulsation which causes poor baseline and decreased precision. Pulsation in this system was largely reduced by regular replacement of the organic-resistant flexible tubing and insertion of a depulse coil between the pump and injection valve. The depulse coil was made from 2 m of 0.8 mm internal diameter (i.d.) polytetrafluoroethylene (PTFE) tubing and acted as an hydraulic buffer. It made no contribution to dispersion of the sample because it was placed prior to the injection valve.

Control of the Alitea peristaltic pumps was facilitated through two external digital connections for direction control and an analog connection (0-10V) for speed control. This voltage was provided by the output of the first 12-bit DAC, and gave a speed resolution of one part in 4095. Alternatively, the speed could be adjusted manually on the front panel of the pump.
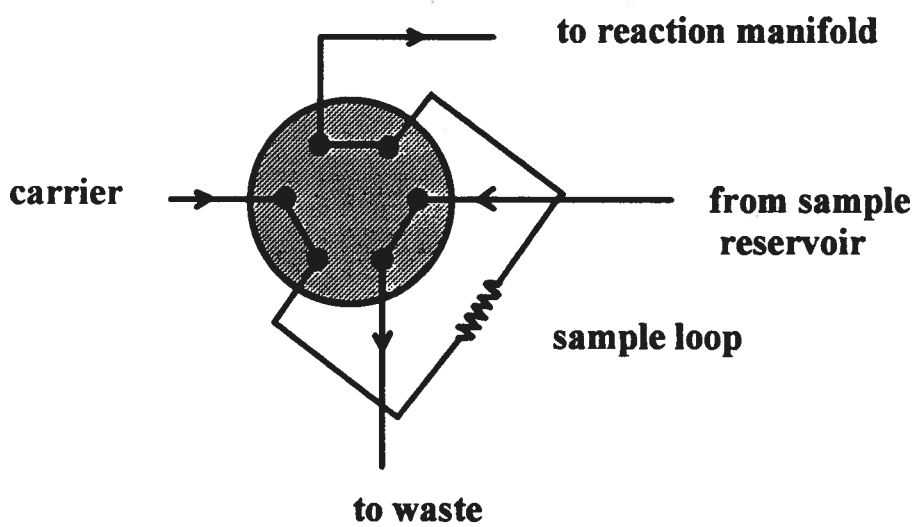
The most suitable tube material for our manifold is PTFE (Teflon®) which, besides being chemically resistant, adsorbs the least solutes onto its surface. Tubing of 0.5 and 0.8 mm i.d. is commonly used in our laboratory. Larger diameter tubing causes increased dispersion while smaller internal diameter tubing can become easily clogged. Other tube materials are polypropylene, polyethylene and trade-name polymer materials such as PEEK® which are highly resistant to organics and strong acids.

2.3.3 INJECTION VALVE

A six-port, air-driven, solenoid-actuated valve (Type 5020P, Rheodyne Inc., Cotati, CA) was selected. This is one of the most commonly used sample injection valves in FIA. Actuator control circuitry was designed by Wentzell *et al* [75]. The operation of such a valve is shown in Figure 2.3. While in the "fill" position, a sufficient amount of sample solution is introduced into a fixed volume loop such that it completely displaces its previous contents. While in this position, the carrier stream by-passes the fixed volume loop and flows directly to the reaction manifold. On switching the valve to the "inject" position (a $60°$ rotation of the 3 internal channels), the carrier stream then sweeps out the contents of the loop, transporting the sample plug downstream. The procedure is repeated as required. Similar designs are used in High Performance Liquid Chromatography (HPLC). The sample loop used in this work was of PTFE tubing of 0.8 mm i.d., 15 cm in length and 75 µl in volume.

to reaction manifold

carrier →

from sample reservoir

sample loop

to waste

FILL

to reaction manifold

carrier →

from sample reservoir

sample loop

to waste
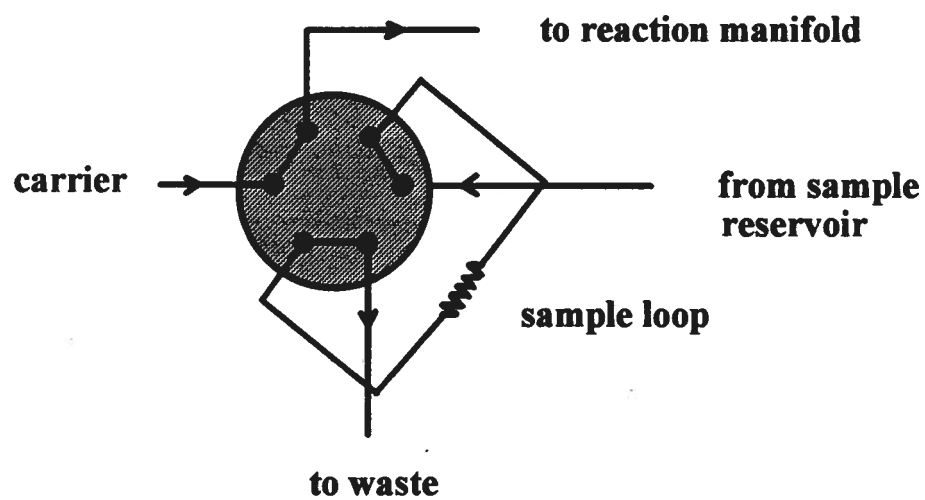
INJECT

Figure 2.3 Internal workings of a six-port injection valve

2.3.4 DETECTORS

Many different types of detectors have been used with FIA systems. These include spectrophotometric (UV, visible and IR), electrochemical (potentiometric and amperometric), mass spectrometric and thermal detectors. The most common of these are UV-visible absorbance detectors, fluorimeters, ion selective electrodes, conductivity detectors, and atomic absorption/emission spectrometers. In addition to obvious criteria such as sensitivity, limit of detection, linearity of response, noise characteristics, peak broadening effects and response time, long-term uninterrupted operation is an important consideration for FIA detectors.

The detectors used in this FIA manifold were a chloride ion selective electrode and a conductivity detector. Free chloride ions are one of the main final products of photodegradation of chloroform. These were monitored quantitatively over a 5.000×10^{-5} to 1.000 M concentration range. Calibration was via a series of standard solutions. Degradation of organics also results in ions other than chloride ions, which increase the conductivity of the solution. Thus, the extent of degradation was monitored by a conductivity detector as well.

The output from one of the detectors was connected directly to the first ADC input of the DACA board. The input voltage range was set at -5V to +5V for the chloride ion selective detector and to -10V to +10V for the conductivity detector. Limitations of the operating software prevented computerized data acquisition from both detectors simultaneously. Therefore, for the experiments in which both detectors were required, the response from the conductivity detector was captured via a chart recorder.

The chloride ion selective electrode (Model 96-17B, Orion, Boston, MA) and its flow-through cell are shown in Figure 2.4. It was developed specifically for measuring chloride in very small samples with minimal flow and measures free chloride ions in aqueous solutions quickly, simply, and accurately. The cell was made in-house from a

block of Teflon®. An amplifier circuit was constructed to match the output range of the ion selective electrode (ISE) to the input range of the ADC. Its very high input impedance also served to avoid current loading of the ISE. It was usually set to provide a gain of 25. The circuit diagram is shown in Figure 2.5.
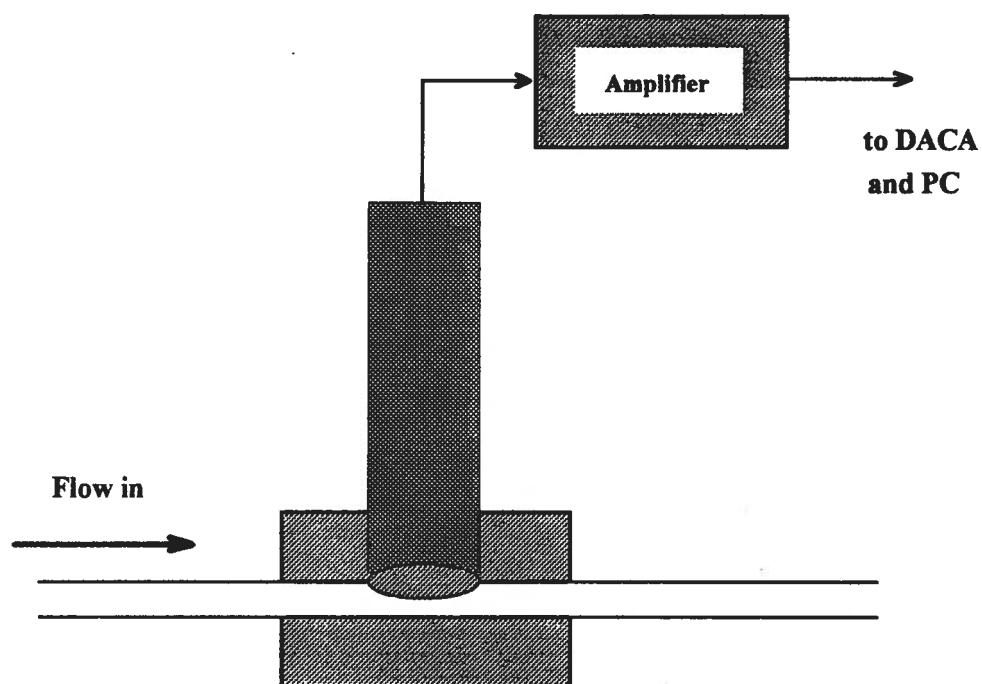

Figure 2.4 Flow through cell with chloride ion selective electrode (Cl⁻-ISE)

POWER SUPPLY

CIRCUIT

Figure 2.5 Circuit of amplifier for chloride ion selective electrode

(The opamps are PMT OP-27E.)

The flow through conductivity detector was made in this laboratory. Its two electrodes are made of platinum. A small ball was made at the end of each electrode to increase the surface area, thereby improving the sensitivity of the detector. It is shown in Figure 2.6. A conductivity-to-voltage converter circuit was also built in this laboratory to facilitate interfacing with the DACA. The circuit diagram for this is shown in Figure 2.7. Resistance R* was set to 100 MΩ, to provide a gain of 10 for our study.
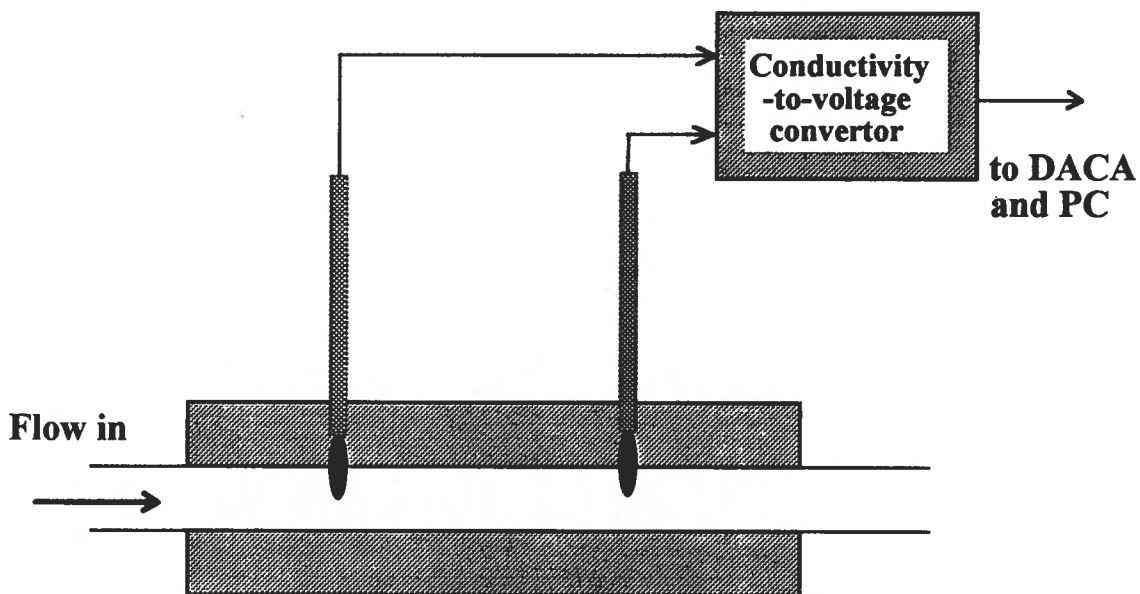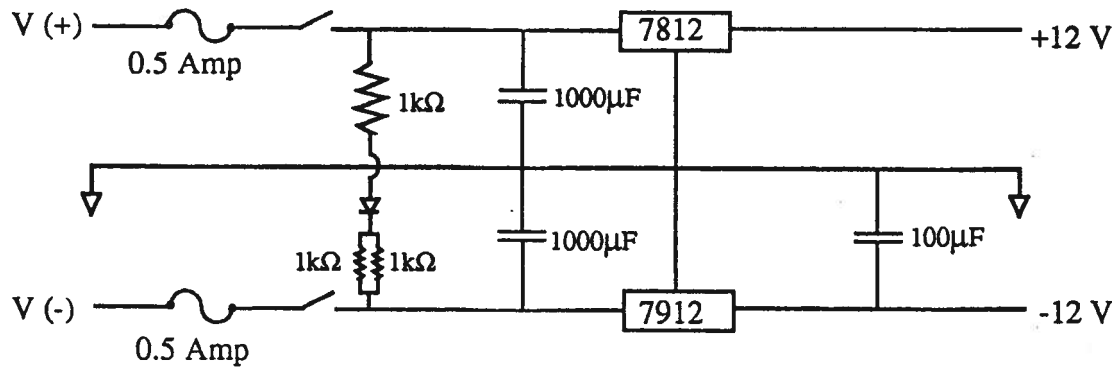

Figure 2.6 Flow-through conductivity detector

POWER SUPPLY

CIRCUIT

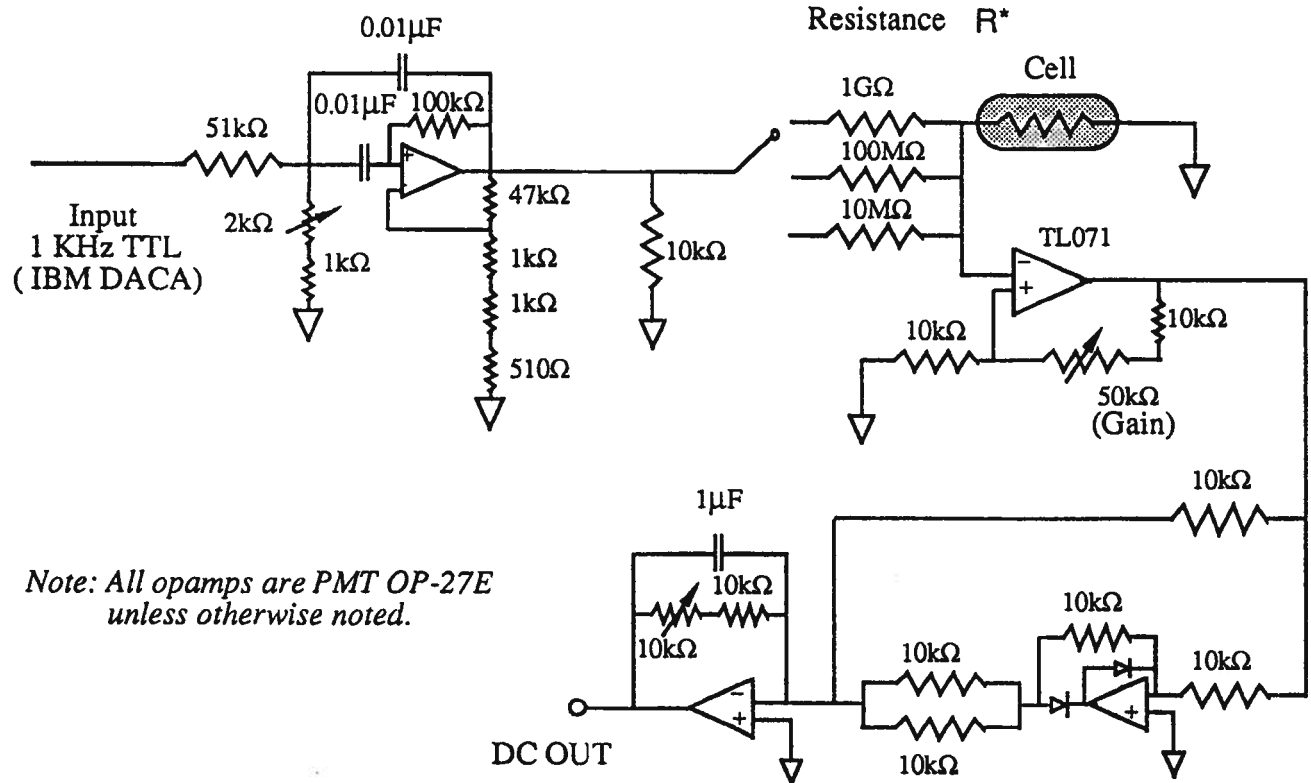*Note: All opamps are PMT OP-27E unless otherwise noted.*

Figure 2.7 Circuit of conductivity-to-voltage converter

40

2.3.5 SIGNAL RECORDING

Historically, chart recorders were used as output devices for FIA. Now microcomputers equipped with a data acquisition card act as an inexpensive digital readout system and are more cost effective and very common. Both are used in this system. The 12-bit analog-to-digital converter (ADC) sampled the detector output at a rate of 5 Hz. These values were plotted versus time on the screen in real-time to display the peak obtained from each injection. The control software then calculated peak height and area, and stored the entire peak data set to disk for later data processing.

2.4 CHARACTERIZATION OF MONITORING SYSTEM

2.4.1 CHARACTERIZATION OF FIA-CONDUCTIVITY DETECTOR AND FIA-CHLORIDE ISE DETECTOR

Figures 2.8a and 2.8b show the relationship plots between the conductivity responses and the concentrations of HCl and KCl for the FIA-conductivity detector. The sensitivities (slopes of the curves) were 11590 ADC units per mmol/l of HCl over the linear dynamic range of 0.0012 to 0.07000 mmol/l for HCl solution and 1590 ADC units per mmol/l of KCl over the dynamic range of 0.05000 to 0.5000 mmol/l for KCl solution. Measurement precisions (relative standard deviations) were 0.59% (n = 5) at 0.06000 mmol/l for HCl solution and 0.26% (n = 5) at 0.5000 mmol/l. Error bars were too small to be seen on the figures.
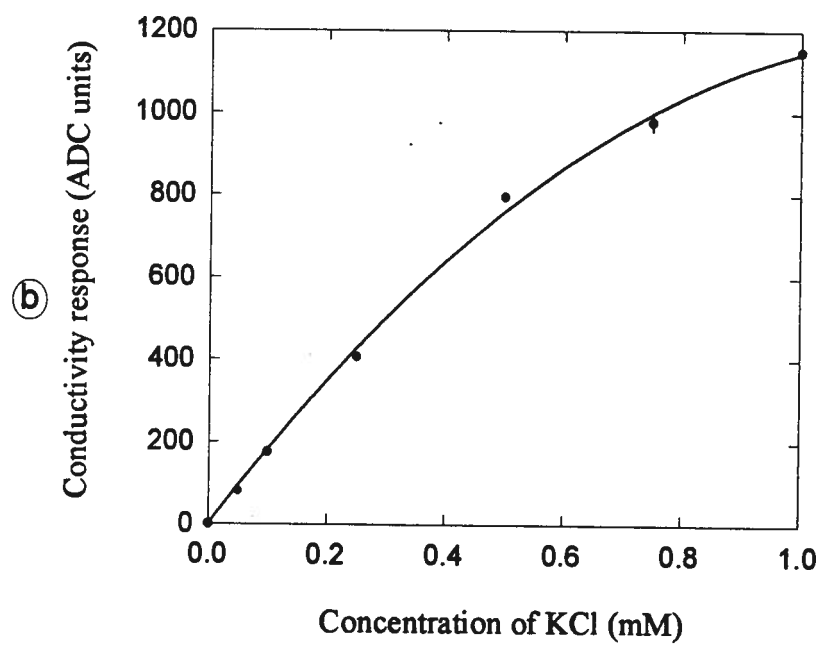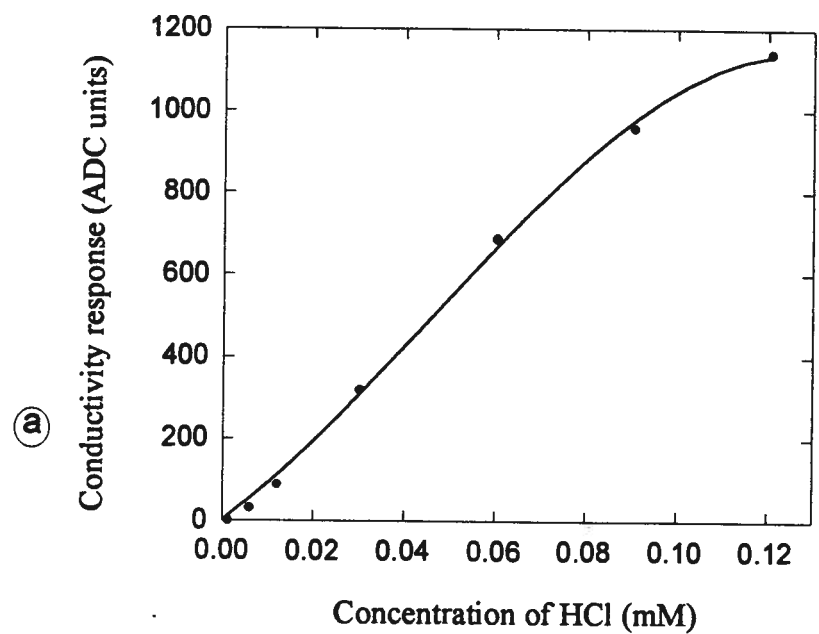
Figure 2.8 Calibration plots for FIA-conductivity detector

The conductivity detector demonstrated a much higher sensitivity for HCl than KCl. Hydrogen ions, when hydrated, are larger than potassium ions and would be expected to be less mobile. The higher mobility of the hydrogen ion is observed only in hydroxylic solvents such as water and the alcohols, in which it is strongly solvated, for example, in water to the hydronium ion, H_3O^+. Thus the H_3O^+ ion is able to transfer a proton to a neighboring water molecule. It is believed to be an example of a Grotthuss type of conductivity, superimposed on the normal transport process.
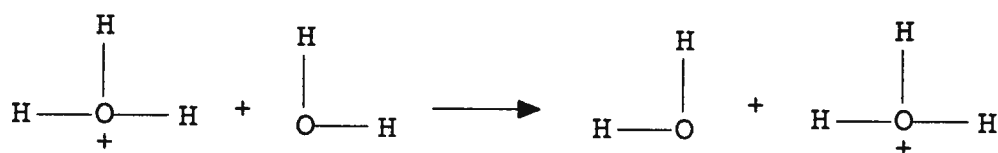
This process may be followed by the rotation of the donor molecule so that it is again in a position to accept a proton. This is the common mechanism for protonic solvents.
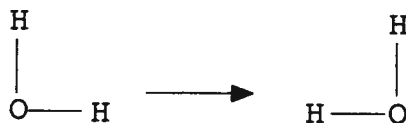
The high mobility of the hydroxyl ion in water is also believed to be caused by a proton transfer between hydroxyl ions and water molecules.
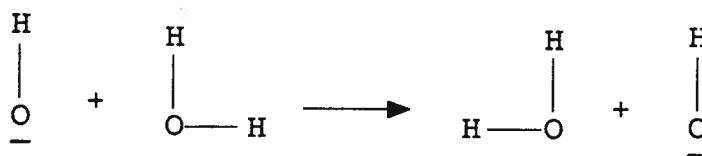
Figure 2.9 shows a calibration plot for the chloride ion selective electrode. The measurement precision was between 0.80% and 5.3% (n = 8) across the linear dynamic range of 5.000 x 10^{-5} to 1.000 mol/l. The electrode had a manufacturer's (Orion

Instruments) rated sensitivity of 56 mV per 10-fold change in concentration of chloride ion. The amplifier circuit used experimentally had a calculated gain of 25, and the output read by the chart recorder was found to be 966 mV per decade. This corresponds to only 39 mV per 10-fold change in concentration of standard solutions of chloride ion injected. The difference could be due to a combination of the following effects: the cross-channel design of the flow cell was such that only 16 % of the electrode surface saw the solution, the observed signals were transients (not steady state), and the electrode saw the peak maximum for less than 5 seconds (a time interval similar to the electrode's expected response time). The peaks observed were skewed Gaussian, rather than flat-topped, indicating that limited dispersion had occurred.
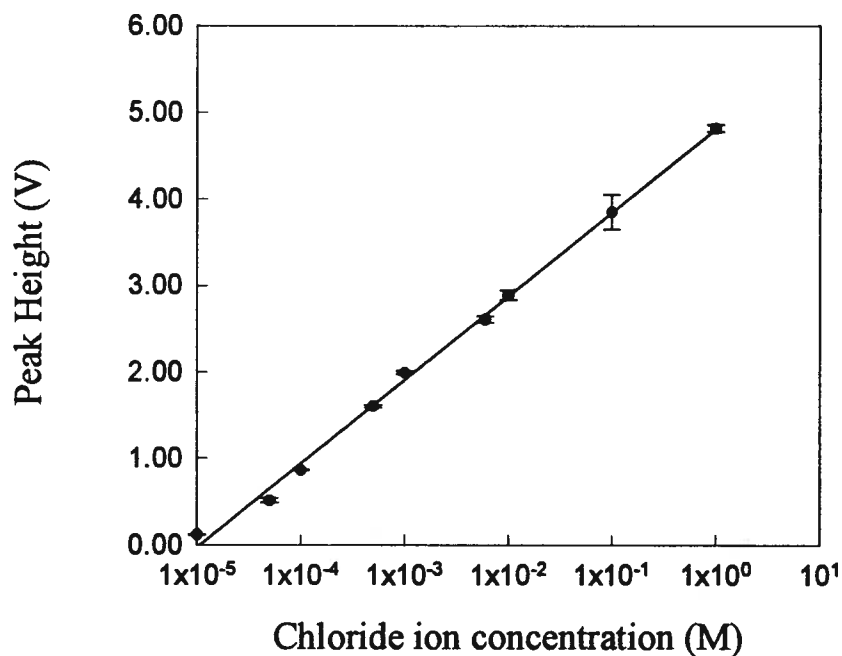

Figure 2.9 Calibration plot for FIA-chloride ISE detector.

2.4.2 REPRODUCIBILITY OF PHOTODEGRADATION-FIA MONITORING SYSTEM

The reactor vessel was loaded with 200.0 mls of solution containing 100.0 ppm initial concentration of chloroform and 0.05 wt% anatase TiO_2 catalyst powder. Photodegradation was used, without sonication. Samples were withdrawn from the reactor by the sampling system and analyzed every 5.5 min for 60 min. Three separate replicate experiments were carried out.

Figure 2.10 shows the average FIA-Cl⁻ ISE monitoring curve for the three replicates, and error bars which provide an estimate of its reproducibility. The variability of results seen is due to less than perfect reproducibility of each of the steps involved: *i.e.*, the photodegradation reaction, sampling, filtration by the in-line microfilter, injection of sample into a flow system, and detection.

The calibration and operation the ISE detector was checked before and after each run using standard potassium chloride solutions of 5.000×10^{-5} M, 1.000×10^{-4} M, 5.000×10^{-4} M, 1.000×10^{-3} M and 3.000×10^{-3} M. The detector was found to maintain its calibration throughout the process.
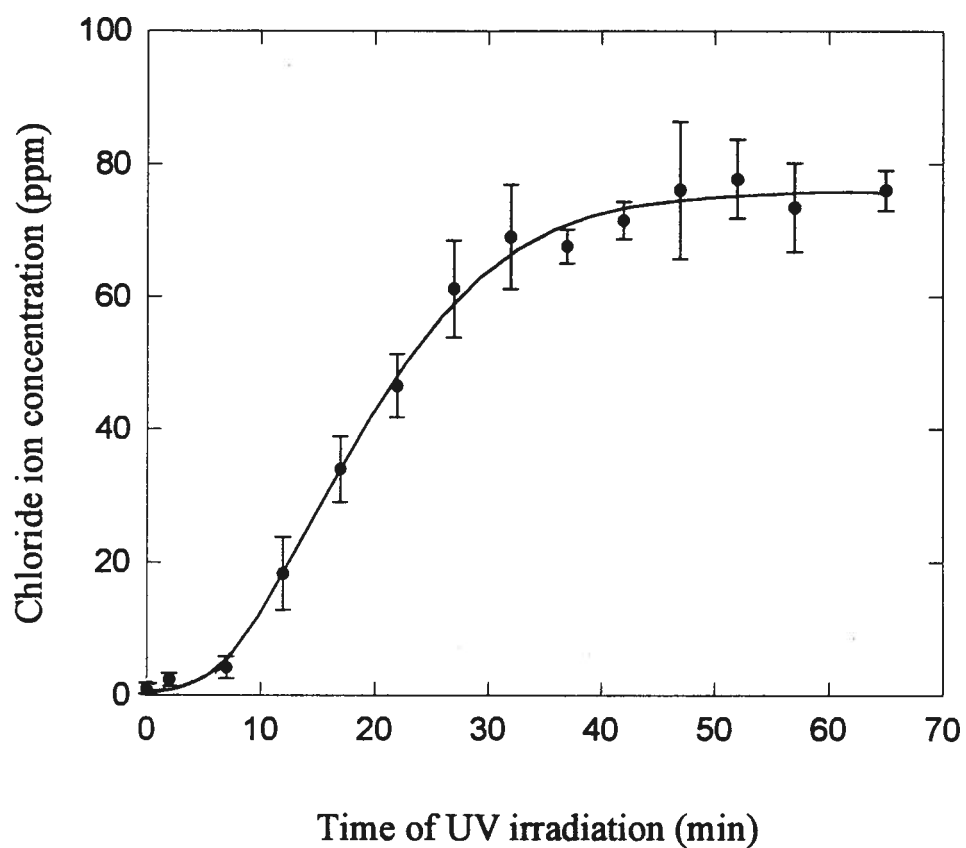
Figure 2.10 Reproducibility of photodegradation-FIA monitoring system (Initial concentration of chloroform: 100.0 ppm; titanium dioxide: 0.05 wt%; error bars are for three replicate experiments)

CHAPTER 3

MONITORING PHOTODEGRADATION OF CHLOROFORM
BY FLOW INJECTION ANALYSIS

Photocatalytic degradation was examined by monitoring the product(s) formed using FIA. Chloroform as a reactant was also monitored off-line by gas chromatography-mass spectrometry (GC-MS). The effects of different amounts of anatase TiO_2 and two forms of TiO_2 were studied, as was the effect of power ultrasound. The kinetics and mechanism of photocatalytic degradation are proposed and discussed in this chapter.

3.1   IN-LINE MONITORING CHLORIDE ION FORMATION BY FIA

To determine the degree and the rate that chloroform is converted from toxic organic chlorine into nontoxic free chloride ions, the formation of chloride ions during the degradation process was monitored with the in-line FIA manifold described in Chapter 2.

The photo-reactor vessel (Figure 2.1) was initially filled with 200.0 ml of 140.0 ppm chloroform solution. A 0.1 gram sample of anatase titanium dioxide powder, corresponding to 0.05 % by weight of the solution, was used as catalyst. While being irradiated with UV light, the degraded chloroform solution in the reactor was sampled into the FIA system every 2.75 minutes. As noted in Section 2.3.4, chloride ions formed in the photodegradation process were quantitatively monitored by using an in-line chloride ion selective electrode (Cl^--ISE) in the FIA manifold (Figure 2.4). Figure 3.1 shows a sample of a series of recorded FIA peaks which reflect the change in chloride ion concentration during the degradation process. The amount of chloride ions liberated is seen to increase

with UV irradiation time over the initial 50 minute span. After that, the peak heights remain at a maximum level, indicating that chloride ions are no longer being produced.
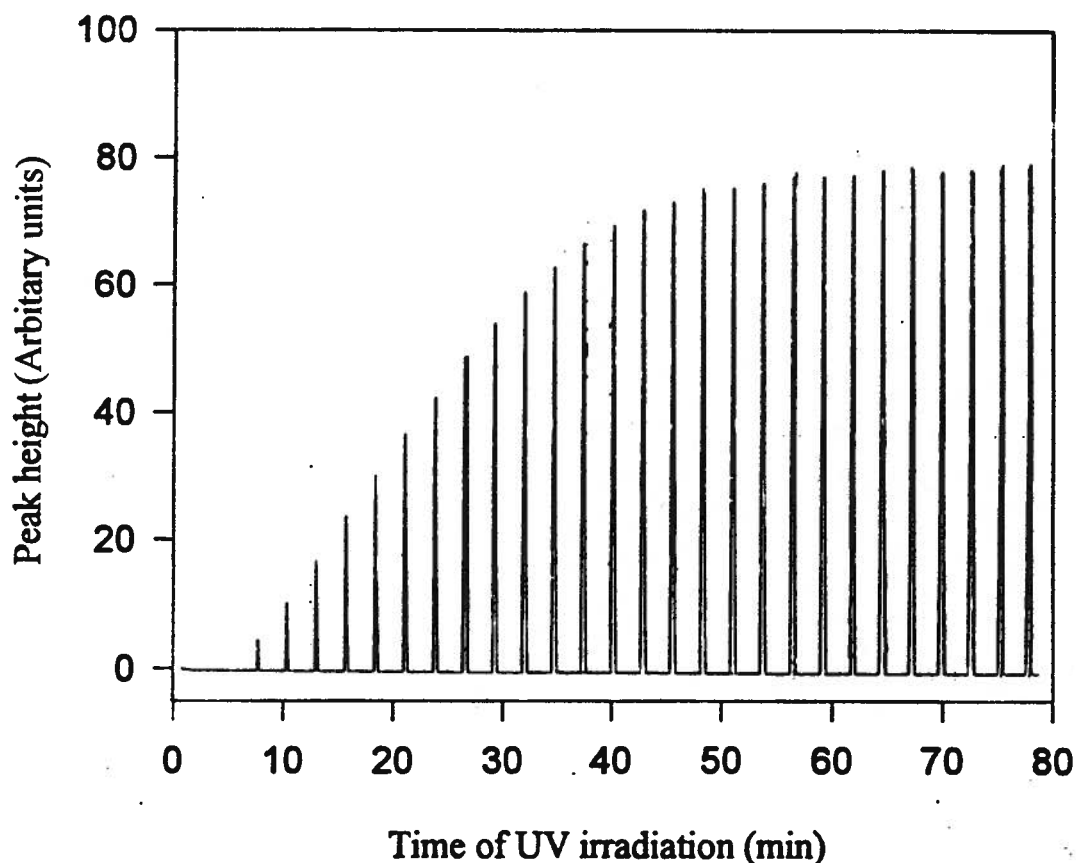
Figure 3.1 Chloride ion peaks recorded with an in-line FIA-chloride ISE detector

The chloride ion concentration corresponding to each peak in Figure 3.1 can be calculated by using a calibration curve prepared prior to each monitoring period. Figure 3.2 shows a curve of chloride ion concentration *vs.* UV irradiation time. For clarity, every other peak from Figure 3.1 is used in Figure 3.2. The maximum chloride ion concentration in the figure is measured to be 122.0 ppm. As summarized in Table 3.1, the 140.0 ppm of original chloroform solution corresponds to a chlorine (Cl) concentration of 124.8 ppm. Therefore, the 122.0 ppm maximum chloride ion concentration obtained corresponds to 97.76 % mineralization of chloroform, *i.e.*, 97.76 % of the organic bonded chlorine has been converted into inorganic free chloride ion.
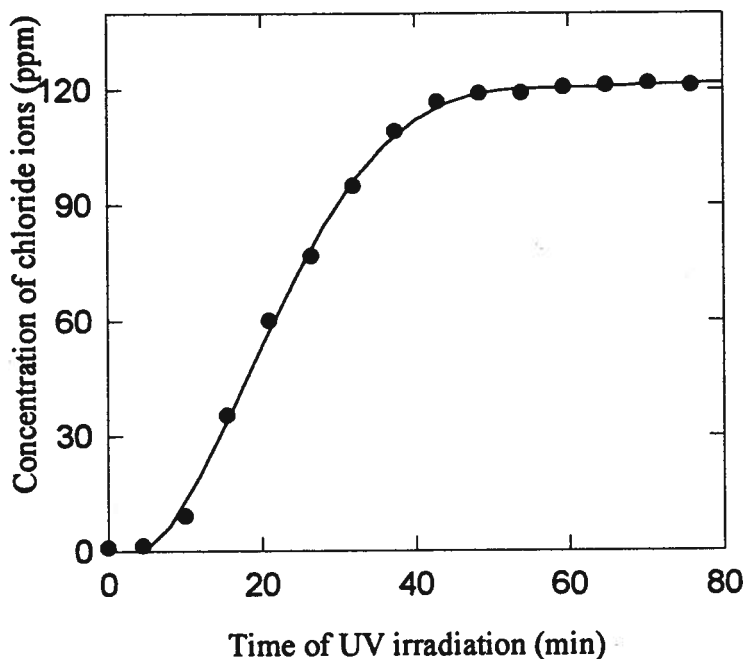
Figure 3.2 Variation of chloride ion concentration with UV irradiation time

Table 3.1 Degree of mineralization of chloroform

Initial concentration of chloroform	140.0 ppm
Initial chlorine concentration [a]	124.8 ppm
Final concentration of chloride ions detected	122 ppm
Degree of mineralization [b]	97.8 %

[a] Initial chlorine concentration = 140 ppm x 3 FW_{Cl} / FW_{CHCl3}

=140.0 ppm x 3 x 35.5/(3 x 35.5 + 13) = 124.8 ppm (FW: formula weight)

[b] Degree of mineralization (%) = 100 * $\dfrac{\text{final concentration of chloride}}{\text{initial chlorine concentration}}$

49

3.2 EFFECT OF TITANIUM DIOXIDE CONCENTRATION ON RATE AND EFFICIENCY OF DEGRADATION

Anatase TiO_2 with a determined BET surface area of 10.8 m^2/g was obtained commercially. In order to examine the effect of titanium dioxide concentration on the rate and the efficiency of photodegradation, five chloroform solutions of the same concentration (560 ppm) were prepared to contain 0.00, 0.01, 0.05, 0.20 and 0.40 weight percentage of TiO_2. UV irradiation was applied to each solution for 80 minutes during which the degradation process was monitored by an in-line FIA-chloride ISE detector. Samples were injected every 2.5 minutes. Figure 3.3 shows how the amount and rate of chloride ions produced are effected by the amount of catalyst used and the time of UV irradiation.
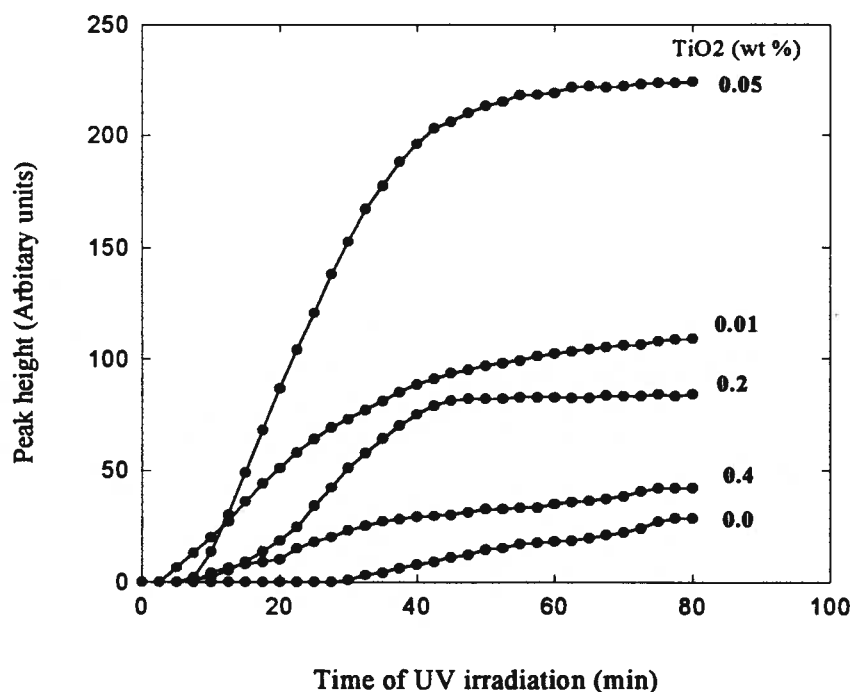

Figure 3.3 The effect of titanium dioxide concentration on rate and efficiency of degradation.

In the absence of photocatalyst, a slow photodegradation curve is observed. Homogeneous reactions occurred under this condition. The energy of UV, provided by the two mercury lamps, might be strong enough to cause breakage of C-Cl bond, but the reaction is not sufficient, nor result in complete destruction of chloroform within a reasonable time period.

When photocatalyst is present, UV irradiation can cause the desired heterogeneous photocatalytic degradation process in addition to homogeneous photolysis reactions. A significant increase in the rate and efficiency of reaction resulted from increasing the concentration of TiO_2 present from 0.0% to 0.05%. A TiO_2 concentration at 0.05 wt% provided the fastest and most efficient destruction. A gradual decrease in rate and efficiency was observed for higher amounts of TiO_2 tried.

Matthews [17] has shown that a dichotomous effect will occur with increasing TiO_2 concentration. At low concentration, the degradation rate can be enhanced by using more catalyst material in order to increase the probability of reaction. The reaction rate increases because more surface area is available for the reactants and because it is more likely that photogenerated electrons and holes will reach the surface of the solid before they recombine. At high concentration, the high opacity and light-scattering properties of the semiconductor limit penetration of the UV light into the solution. Moreover, aggregation of catalyst particles may also reduce the available surface area.

Tominaga et al [75] demonstrated that the oxidation rate of an organic solute on a photocatalyst is proportional to the fraction of the surface of the semiconductor covered by the solute molecules. At low solute concentrations, there is an overabundance of adsorption sites available to the solute and any further increase in number of sites would not significantly increase the rate of photocatalytic oxidation. In contrast, for solutions of higher concentration, sites are available for only a fraction of the total solute present and this limits the photooxidation rate. An increase in the number of adsorption sites will

therefore increase the rate of oxidation for solutions of higher concentration (subject to the limitations discussed above).

3.3   STUDY ON TWO DIFFERENT TYPES OF TIO$_2$ CATALYSTS

The anatase modification of TiO$_2$ in the form of powder suspended in water shows promise as a photocatalyst for the photodegradation of organic contaminants in water. Since this powder is very fine and light, it must be filtered before analysis can be performed with the FIA system. This inconvenience has prompted the author to make a preliminary investigation into the use of amorphous TiO$_2$ in the form of a porous glass. The high surface area of porous glassy TiO$_2$ makes it suitable for photocatalytic applications. Glassy TiO$_2$ exists in the form of small pieces of glass and does not need separation prior to the detection. Porous glassy TiO$_2$ has been used as a photocatalyst for hydrogen production from water [79]. No papers have reported its use in photodegradation of aqueous organic impurities.

The glassy TiO$_2$ was provided by Dr. Gesser of the Chemistry Department, University of Manitoba. It was prepared by a slow low-temperature hydrolysis of TiCl$_4$, followed by partial removal of HCl and partial neutralization by the addition of KOH. Dialysis of the solution resulted in the formation of a gel which shrank as it dried to a transparent porous glass which was then annealed (79, 80). The glassy TiO$_2$ is in the shape of flat wafers 0.5-1 mm thick and up to 3.5 mm in diameter. Its BET surface area was determined to be 91.6 m^2/g.

In this experiment, three solutions with 700 ppm concentration of chloroform were prepared, and run in series. 0.0, 0.2 g of glass and 0.2 g of anatase TiO$_2$ powder were added to separate solutions. Samples were analyzed every 1.5 minutes. Photodegradation was monitored for 45 min. Conductivity responses were recorded on a chart recorder.

Figure 3.4 shows the recorded peaks for each set of experimental conditions. All the peaks were plotted using the same scale.

Reaction without catalyst is slow. It has a different reaction route. The mechanism of photodegradation solely by UV irradiation involves homogeneous reactions or bond cleavage caused by the high energy of UV light. When catalyst was added to the solution, efficiency was enhanced. The reaction involves electrons, holes, and HO· radicals as intermediates which have a much higher reactivity. With a same weight concentration (0.1%), anatase TiO_2 acts about four times more efficiently than glassy TiO_2. The first step of the reaction involves the movement of chloroform molecules to reach the TiO_2 surface by diffusion. The size of glass is much larger than powder, thus only a few pieces of glass were used in 200 ml solution while anatase TiO_2 was suspended throughout the solution. Therefore, in glassy TiO_2 catalyst solution chloroform molecules have to travel a longer distance on average to reach the catalyst. Further, most of the surface area is already saturated by water molecules before the chloroform reaches them because water is much more concentrated and polar than chloroform. A greater number of chloroform molecules are in the immediate vicinity of anatase TiO_2 particles since these particles are suspended everywhere in the solution. Therefore the anatase TiO_2 had a larger chance of reaction than glassy TiO_2, even though the glassy TiO_2 has a much larger measured BET surface area.

This study shows the potential of glassy TiO_2 in photodegradation of aqueous organic impurities. Increasing the amount of glass and decreasing its size may improve the efficiency of photodegradation significantly. This should be studied in the future. Using glassy TiO_2 is one way to solve the separation problem which exists when using the anatase form. The system could be simplified from "photodegradation-filtration-FIA monitoring" to "photodegradation-FIA monitoring".
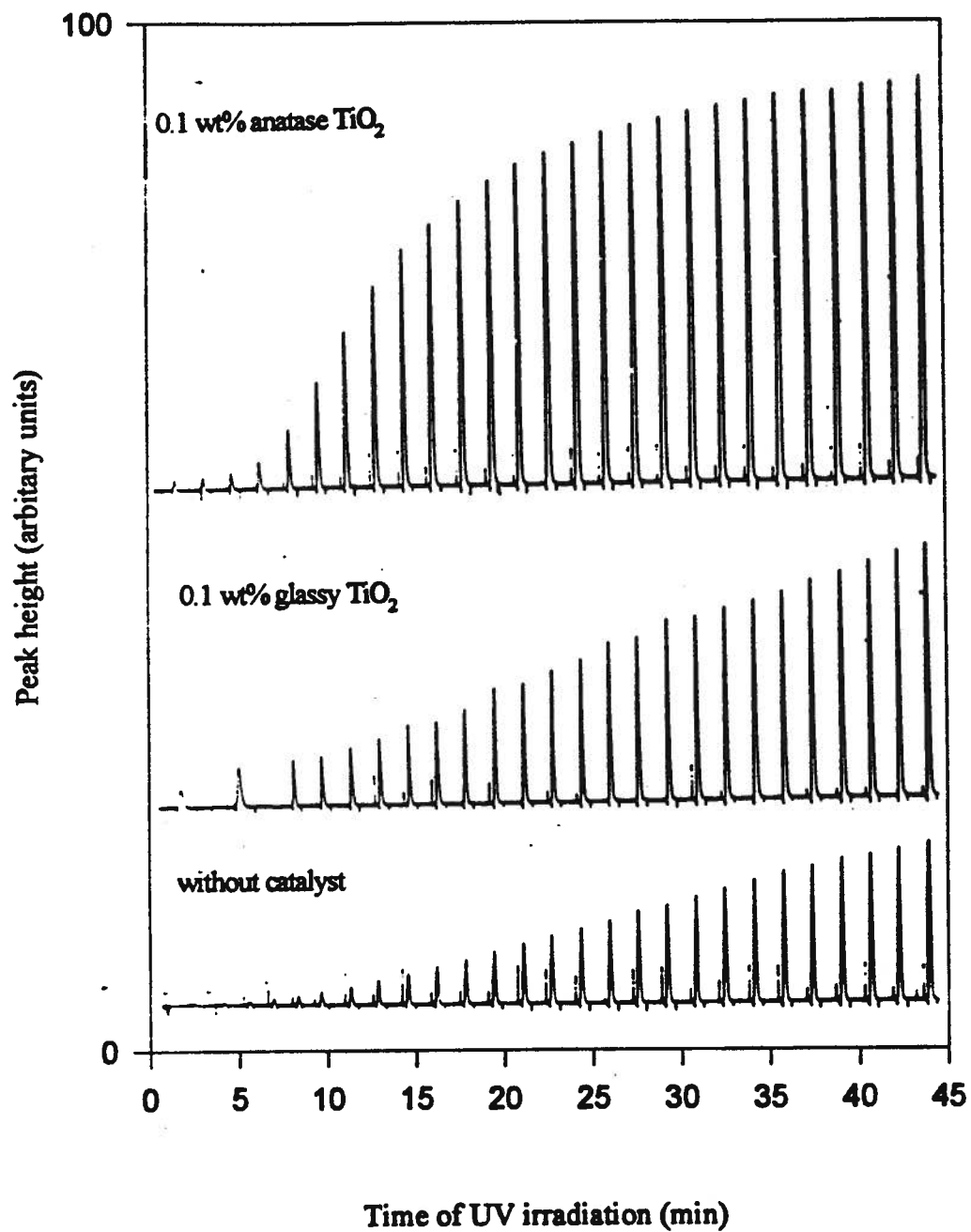
Figure 3.4. Comparison of the efficiencies of two different forms of TiO$_2$ catalyst.

(1.5 minutes between sample injections)

3.4 COMPARISONS OF EFFICIENCIES OF PHOTODEGRADATION BY USING DIFFERENT CONDITIONS IN THE REACTOR CELL

Addition of power ultrasound did not affect the photodegradation of homogeneous chloroform solution. For the study of power ultrasound, a heterogeneous solution was prepared by adding 1.00 ml of chloroform to deionized water and making up to 200.00 ml. The solution had two layers because the chloroform did not completely dissolve. Six different conditions of the reactor cell were examined. These were: (1) testing of the blank solution itself; (2) anatase TiO_2 catalyst (0.1 wt %), (3) UV irradiation; (4) UV irradiation with anatase TiO_2 catalyst (0.1 wt %); (5) power ultrasound; and (6) the combination of UV irradiation, catalyst and power ultrasound. Replicate chloroform solutions were prepared for the study of each of the different conditions. UV light and/or power ultrasound were turned off at different times and the degraded chloroform solution under each condition was sampled and analyzed for three replicates. Signals obtained were recorded using chart recorders. Figure 3.5a shows the conductivity response and figure 3.5b shows the chloride ion selective electrode response obtained after degrading for 20 minutes.

To establish that chloroform solution does not degrade on its own in water, a chloroform solution which did not contain any catalyst, and was subjected to neither ultrasonic nor UV irradiation, was also studied. Samples were propelled without passing through the micro filter. It was found that no ions were produced during the first 20 minutes.

Chloroform solution containing TiO_2 catalyst gave tiny signals at both detectors. The signals did not increase with time. Therefore, chloroform did not degrade in the presence of catalyst only. The small signals detected resulted from a very small amount of ions from impurities contained in TiO_2 powder or the 0.22 μm microfilter.
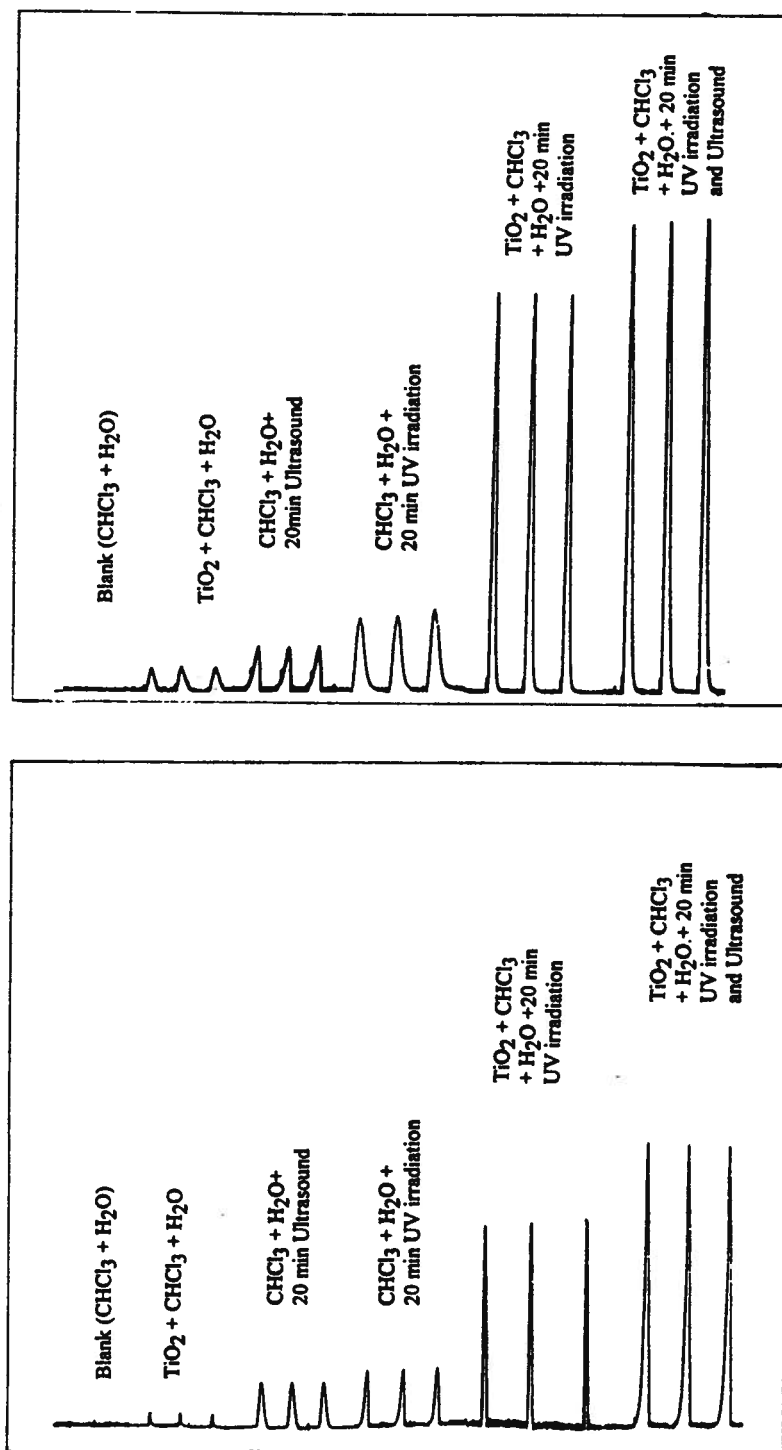
55

Figure 3.5 Recorded FIA peaks after 20 minute degradation with each different conditions. (a) FIA-conductivity responses, (b) FIA-chloride ISE responses.

UV illumination of aqueous solutions of chloroform in the presence of suspended titanium dioxide caused a rapid degradation. UV irradiation causes homolytic cleavage of the C-Cl bond of chloroform. Hydroxyl radicals, HO·, produced from TiO_2 catalyst irradiated with UV light cause rapid destruction of chloroform. In the presence of UV illumination without TiO_2, or in the presence of ultrasound only, very slow degradation was observed. Combined sonolysis and catalyzed photolysis provided the most efficient degradation of chloroform and the yield was improved by about 41% based on the detection of chloride ions.

The effects of power ultrasound on the degradation of chloroform are discussed below.

*Direct sonolysis of chloroform:*

Chloroform may be directly decomposed by irradiation with power ultrasound. When an aqueous medium containing organic halogen compounds (*e.g.*, CH_2Cl_2, $CHCl_3$ or CCl_4) is irradiated with ultrasound, the extreme energy of power ultrasound can cause cleavage of the carbon-halogen bond [31].

A very detailed study has been made of the decomposition of chloroform by the irradiation of power ultrasound [81]. Homolysis occurs yielding a large number of products among which are HCl, CCl_4 and C_2Cl_4. One of the products of sonolysis of chloroform, HCl, can be detected by both a conductivity detector and a Cl^--ISE detector. The precise mechanism involved in the decomposition is complex but almost certainly involves the homolytic fission of chloroform to radicals and the formation of carbenoid intermediates as shown in scheme 3.1 [82].
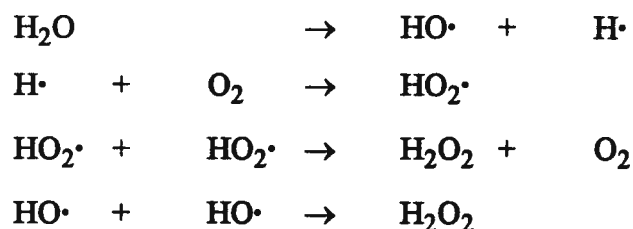
$$CHCl_3 \rightarrow \cdot CHCl_2 + \cdot Cl$$
$$\rightarrow \cdot CCl_3 + H\cdot$$
$$\rightarrow :CCl_2 + HCl$$
$$\rightarrow :CHCl + Cl_2$$
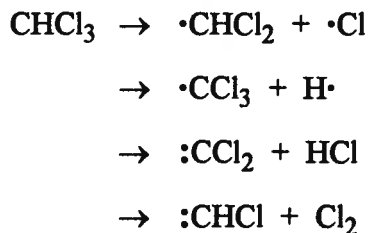
Scheme 3.1 Decomposition reactions of chloroform

Evidence for the generation of these reactive intermediates was obtained from a study of the effect of added cyclohexene (1) on the sonication of chloroform [82]. The presence of free radicals in the system was confirmed by the appearance of chlorocyclohexane as a product and by the increase rate of decomposition of chloroform in the presence of cyclohexene. Carbene intermediates are implicated by the formation of three member ring compounds such as (2) via dichlorocarbene addition to cyclohexene.

(1)   (2)
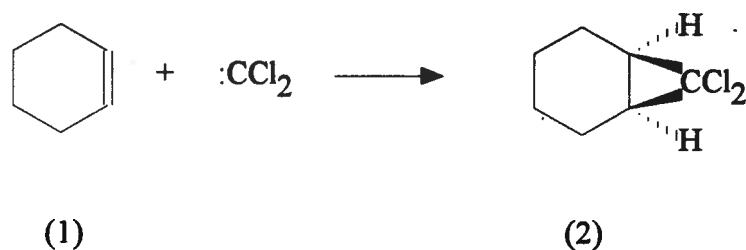
A second important factor is the generation of active intermediates — HO· radicals from water. When water is sonicated, extreme conditions are generated by collapse of the cavitation bubbles. These are sufficient enough to cause the rupture of the O-H bond itself with formation of highly reactive radical species and subsequent production of oxygen gas and hydrogen peroxide (Scheme 3.2) [34]. The ultrasonically produced HO· radicals are very important in the photodegradation of organic impurities. Any species dissolved in the water are clearly going to be subject to chemical reactions with these ultrasonically produced HO· radicals and/or hydrogen peroxide HO_2·. Organic compounds can be degraded in this environment, and inorganic compounds can be oxidized or reduced.

$$H_2O \rightarrow HO\cdot + H\cdot$$

$$H\cdot + O_2 \rightarrow HO_2\cdot$$

$$HO_2\cdot + HO_2\cdot \rightarrow H_2O_2 + O_2$$

$$HO\cdot + HO\cdot \rightarrow H_2O_2$$

Scheme 3.2. The decomposition of water by power ultrasound

Sonochemical photodegradation of chloroform:

When power ultrasound irradiation was combined with catalytic UV irradiation, an enhanced degradation efficiency was obtained. Some factors which may contribute to this effect are as follows:

(1)   Reaction was promoted by improving the activity of the catalyst powder.

Solid catalysts suffer from surface deactivation through chemical contamination (poisoning) and passivation during continuous usage. The cleaning effect of ultrasound and its surface activation are important in the enhancement of catalytic reactions. Ultrasound also increases movement of fresh solution to the catalyst surface. When the catalyst is in the form of a powder like anatase TiO_2, power ultrasound can also be used to increase its dispersion in solvents and reduce the particle size, thereby increasing the available surface area for reaction. Thus, the activity of TiO_2 powder as catalyst in the photodegradation study was improved by sonication.

(2)   Sonication generated an extremely fine emulsion, resulting in very large interfacial contact areas between the two layers. More chloroform molecules contacted the aqueous solution where photodegradation occurred. The vigorous mechanical vibration from ultrasound enhanced the transfer of chloroform molecules from organic to aqueous layer, thus increasing the reactivity.

(3) Photodegradation reaction was further facilitated by the localized high temperatures and pressures associated with cavity implosion near the catalyst surface.

3.5 OFF-LINE QUANTITATIVE ANALYSIS OF RESIDUAL CHLOROFORM

The decrease in chloroform concentration during the degradation process was monitored by using gas chromatography-mass spectrometry (GC/MS). Samples of chloroform solutions were taken from the photo-reactor (Figure 2.1) at different UV irradiation times and stored in glass vials without headspace at 4°C in a refrigerator for several days until GC-MS instrument time was available. Each of these degradation samples was introduced into the GC column via a purge and trap procedure. To minimize the effects of run-to-run changes in instrument performance or execution of the purge and trap technique, C_6D_6 was added into each sample as an internal standard and detected together with chloroform.

To dilute the sample solution, 1.0 µl C_6D_6 (20 ppb) internal standard and 100.0 µl of chloroform sample solution were added to deionized water and made up to 5.00 ml. This aqueous sample was then purged by Helium gas and the resultant effluent was allowed to pass through a gel column which adsorbed the purged organics. The trapped organics were then desorbed into the GC column where chloroform and the internal standard were separated. The GC effluents were finally analyzed by a mass spectrometer equipped with an electron impact ionization source.

Figure 3.6a shows a sample total ion current (TIC) chromatography detected by GC/MS. The small TIC peak corresponds to C_6D_6, as verified by the mass spectrum extracted from the peak. Figure 3.6b shows the mass spectrum extracted from the large TIC peak; it matches the standard mass spectrum of chloroform. Therefore, the large TIC peak in Figure 3.6a corresponds to chloroform, the only major component that was purged from the sample solution.
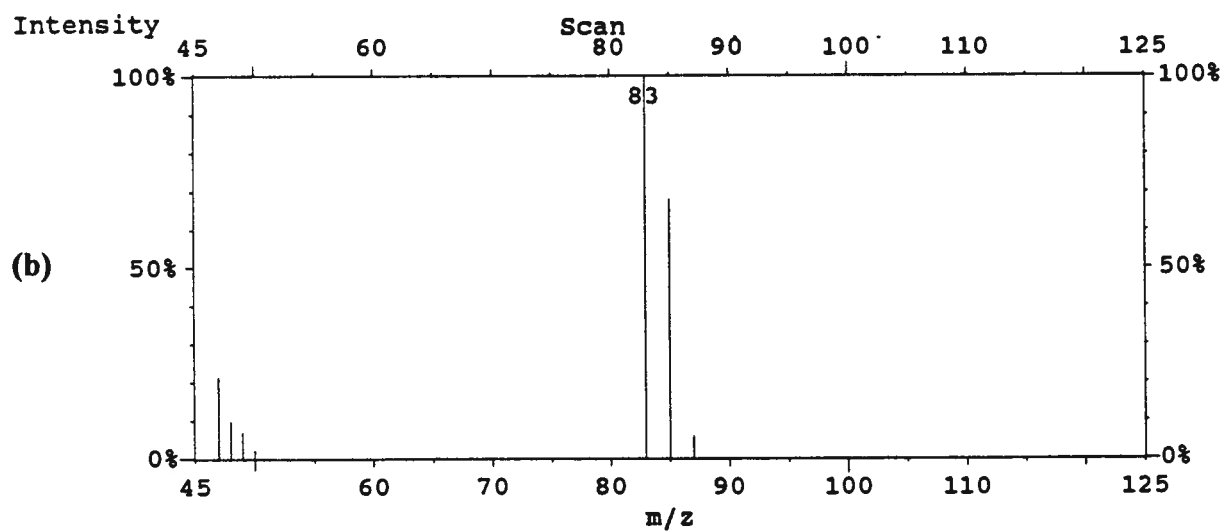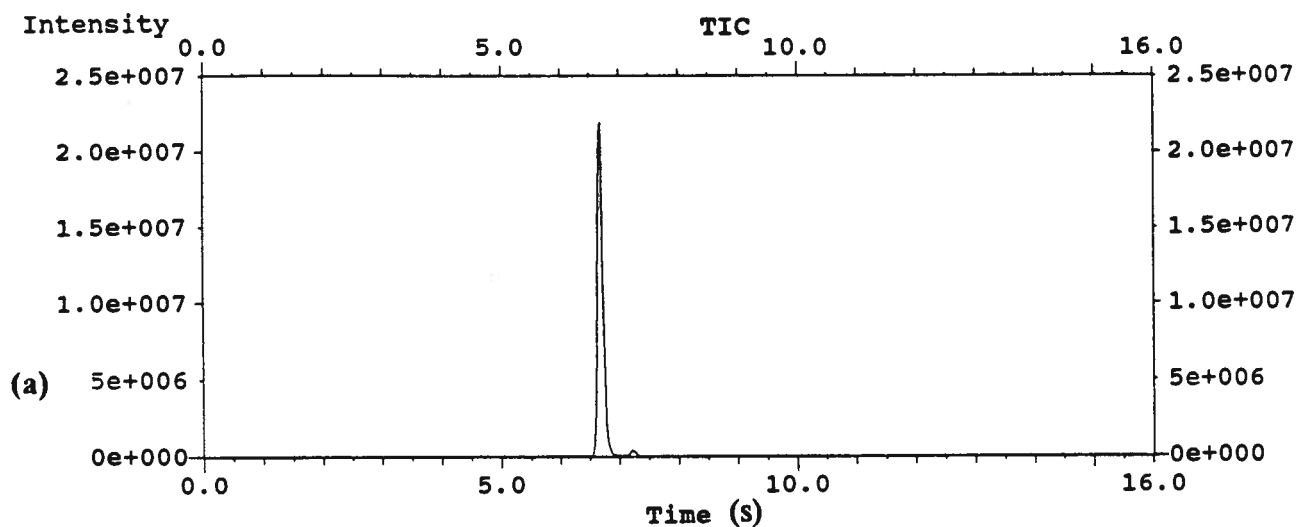
Figure 3.6 (a) Total ion current chromatogram of partially degraded sample.

(b) Mass spectrum of chloroform.

In order to determine the concentration of chloroform in each degradation sample, a series of calibration solutions were prepared in a similar way in which the sample solutions were prepared. Internal standard was added to both the calibration solutions and to the degradation samples. Any changes in the instrument conditions affect the response of analyte and internal standard in the same way. Therefore, the ratio of chloroform response (peak area) to that of the internal standard will not be affected by measurement fluctuations in the GC/MS system. The relative response factor (R) is used to build the relationship between internal standard and standards or analytes in samples and is defined as:

$$R = (C_{std} \; A_{Istd}) \, / \, (C_{Istd} \; A_{std})$$

where C_{std} is the concentration of the sample standard ($CHCl_3$), C_{Istd} is the concentration of the internal standard (C_6D_6), A_{std} is the peak area of the sample standard and A_{Istd} is the peak area of the internal standard. The relative response factor is a constant. In this experiment, all the calibration solutions prepared had the same concentration of C_6D_6, and therefore the ratio of peak area of standard to that of internal standard was proportional to the concentration of standard. In the mass spectrum of benzene-d_6, the molecular ion $C_6D_6^+$ (m/z 84) gives the base peak. As noted in Figure 3.6b, $CHCl_2^+$ (m/z 83) is the most abundant ion in the mass spectrum of chloroform. In this study, the ratio between the peak area of $CHCl_2^+$ and that of $C_6D_6^+$ for each calibration sample was used to prepare the calibration curve shown in Figure 3.7. The $CHCl_2^+$-to-$C_6D_6^+$ ratio was then calculated for each degradation sample to determine the concentration of chloroform.
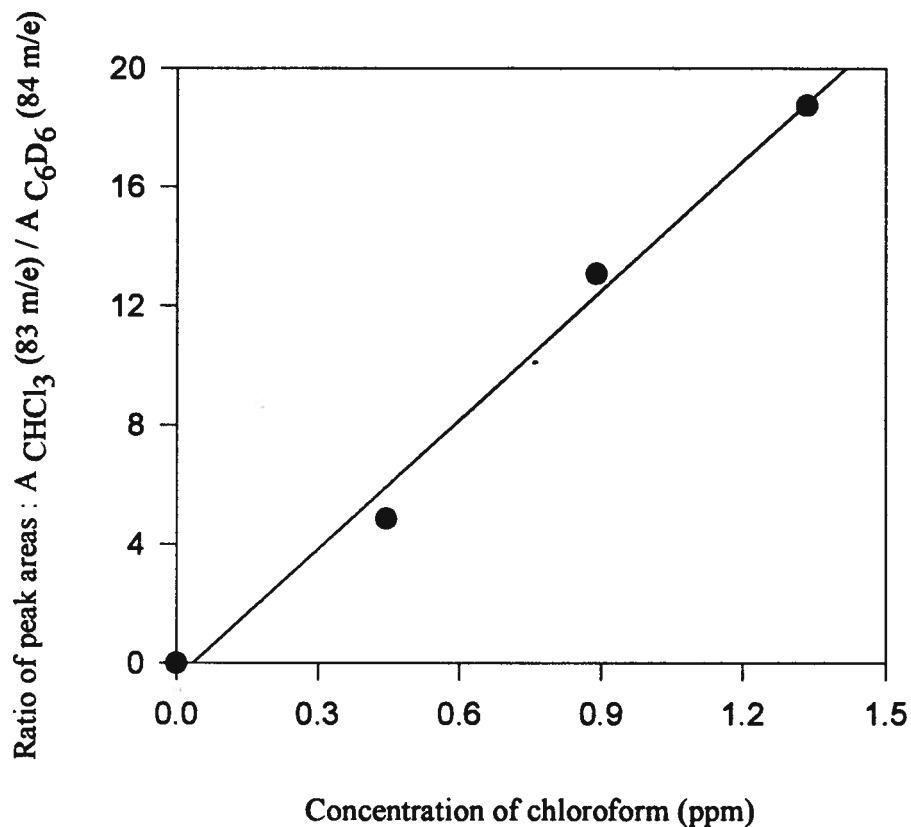
Figure 3.7 Calibration curve of chloroform

The concentration of chloroform for each degradation sample taken at a different UV irradiation time was measured. The disappearance curve of chloroform with irradiation time is shown in Figure 3.8. Chloroform was rapidly degraded and the percentage converted at 44 minutes was about 94%, which is compatible with the value obtained by monitoring the formation of chloride ions (Figure 3.2).
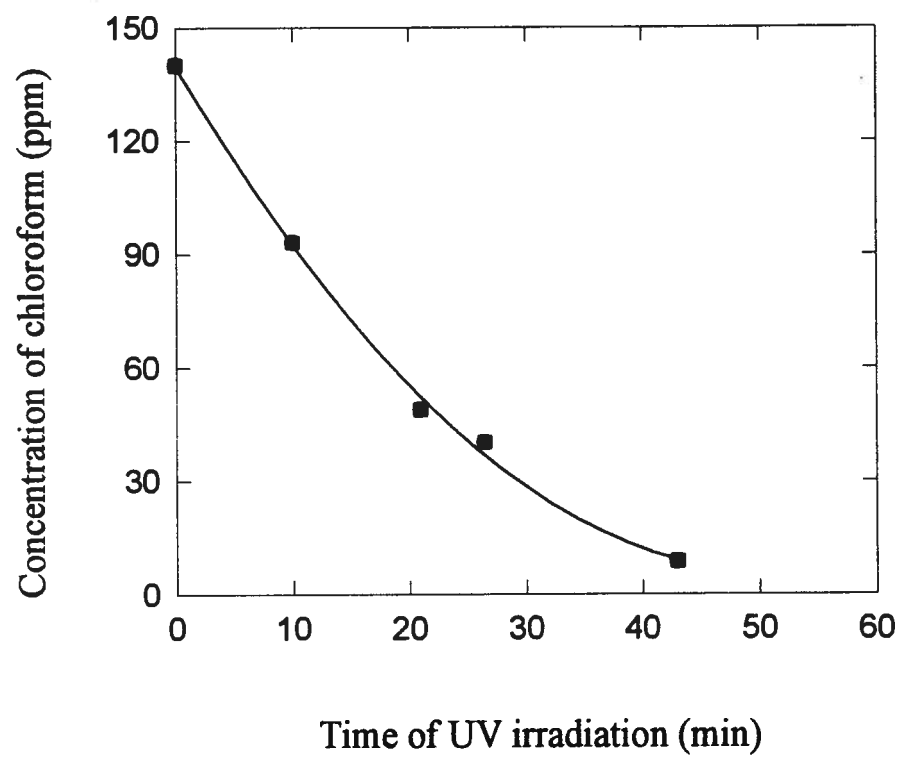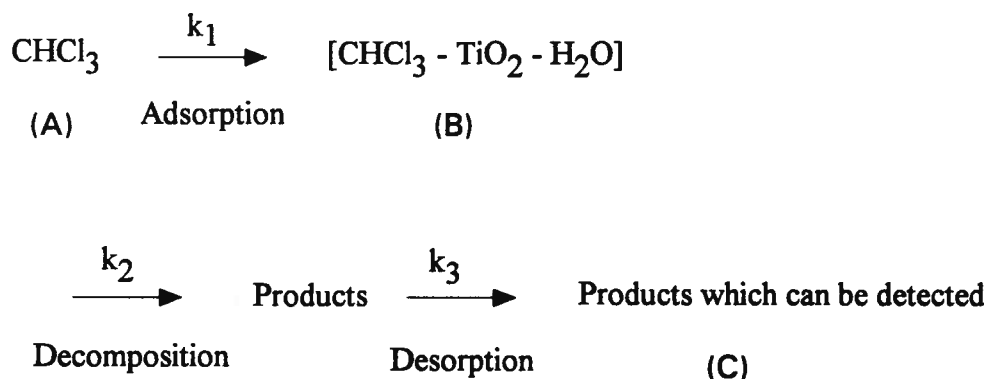
Figure 3.8 Disappearance of chloroform

3.6 MECHANISM AND KINETICS OF PHOTOCATALYTIC DEGRADATION

Figure 3.9 shows the disappearance curve of chloroform and the appearance curve of chloride ions plotted using the data from sections 3.1 and 3.5. Chloroform disappears exponentially with UV irradiation time, which indicates a first-order decomposition.

Assuming that the first-order decomposition of chloroform directly yields chloride ions, i.e., the reaction follows an A → B' kinetic model (A is a reactant, B' is a product), the appearance of Cl⁻ would follow the dotted curve indicated in Figure 3.9. Instead, the formation rate of Cl⁻ at shorter times is slow and then increases significantly until the concentration of Cl⁻ reaches the maximum level. This formation pattern resembles an A → B → C consecutive first-order reaction (A is a reactant, B is an intermediate product, C is a final product), with Cl⁻ being the final product. Accordingly, this author proposes the following mechanism for catalyst-assisted photodegradation of chloroform.

$$CHCl_3 \xrightarrow{\ k_1\ } [CHCl_3 - TiO_2 - H_2O]$$

(A)   Adsorption   (B)

$$\xrightarrow{\ k_2\ } \text{Products} \xrightarrow{\ k_3\ } \text{Products which can be detected}$$

Decomposition   Desorption   (C)

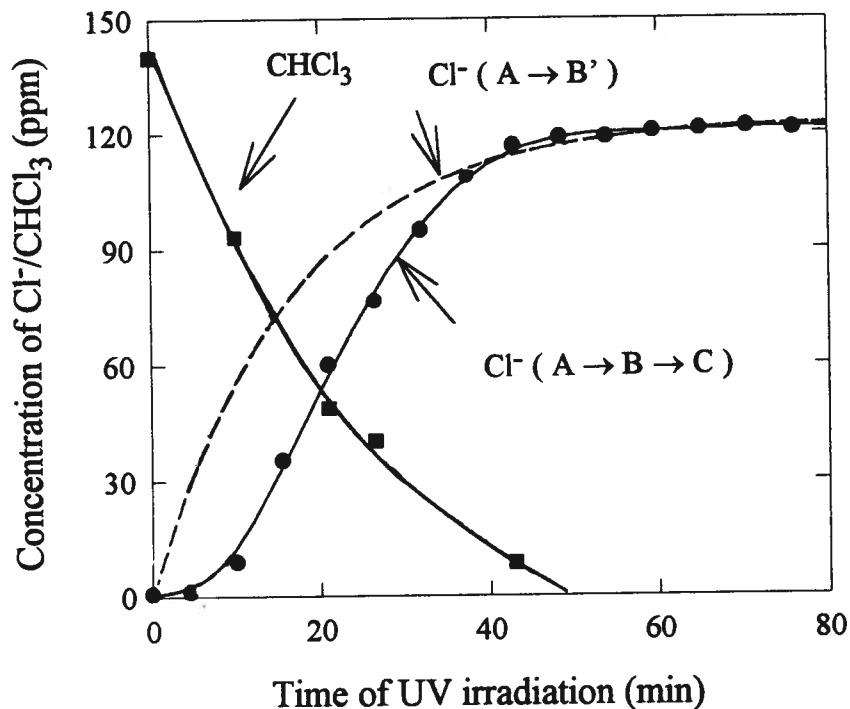**Scheme 3.3** Three steps of photocatalytic degradation of chloroform.

Figure 3.9 Variations of the concentrations of CHCl₃ and Cl⁻ *vs.* UV irradiation time. The dotted curve is manipulated by assuming an A→ B' reaction mechanism from CHCl₃ to Cl⁻.

The whole degradation process is believed to involve three major steps: *(Step 1) adsorption of chloroform on the surface of TiO₂, (Step 2) decomposition of chloroform on the surface of TiO₂ and, (Step 3) desorption of products from the surface of TiO₂.* Steps 1 and 2 are slow and determine the rate of the overall reaction, *i.e.* the formation rate of chloride ions. Therefore, the reactions correspond to the A → B → C series reactions, which is consistent with the appearance curve of chloride ions indicated in Figure 3.9 by filled circles.

Assuming that the process corresponds to the simplest first-order consecutive reactions: A undergoes a first-order reaction to give B, which in turn undergoes a first-order reaction to give C, back reactions are neglected. The system can be represented as:

$$A \xrightarrow{\ k_1\ } B \xrightarrow{\ k_2\ } C$$

in our case, k_1 is the rate constant of the adsorption reaction, k_2 is the overall rate constant of the decomposition reaction. The rate of disappearance of A is given by

$$-d[A]/dt = k_1[A]. \qquad (1)$$

The rate of appearance of B is given by

$$d[B]/dt = k_1[A] - k_2[B]. \qquad (2)$$

and that of C by

$$d[C]/dt = Rk_2[B] \qquad (3)$$

where [A], [B] and [C] are concentrations in ppm units, R is the ratio of chlorine in chloroform.

It is to be noted that

$$d[A]/dt + d[B]/dt + d[C]/(Rdt) = 0; \qquad (4)$$

this is necessary since the sum of the concentrations of A, B, and C must remain constant throughout the degradation process.

Equation (1) may be integrated at once to give

$$[A] = [A_0] \, e^{-k1t} \qquad (5)$$

where $[A_0]$ is the initial concentration of reactant which is 140 ppm.

Equation (2) can be integrated by inserting equation (5) to give

$$[B] = [A_0] \{ k_1 / (k_2 - k_1) \} \{ e^{-k1t} - e^{-k2t} \}. \qquad (6)$$

The rate of change of C is readily found using the fact that

$$[C] = R([A_0] - [A] - [B]), \qquad (7)$$

which leads to

$$[C] = R [A_0] \{ 1- (k_2 e^{-k1t} - k_1 e^{-k2t}) / (k_2 - k_1)\} \quad (8)$$

or $\quad [C] = [C_f] \{ 1- (k_2 e^{-k1t} - k_1 e^{-k2t}) / (k_2 - k_1)\} \quad (9)$

where the final concentration of chloride ion, C_f is 125 ppm.

According to the equation (5), the variation of [A] with time in Figure 3.8 is shown schematically in Figure 3.10 (fitted curve). It was obtained from the curve fitting program (Jandel Sigma Plot for Window, Version 1.0), using k_1 as a fitted parameter. The k_1 value was calculated as 0.0488 min^{-1}. The mean value of the sum of square errors (MSSE = Σ $(X_e - X_c)^2/N$, X_e, experimental value; X_c, calculated value; and N, number of points) of the fitted curve was 26.13 ppm^2.
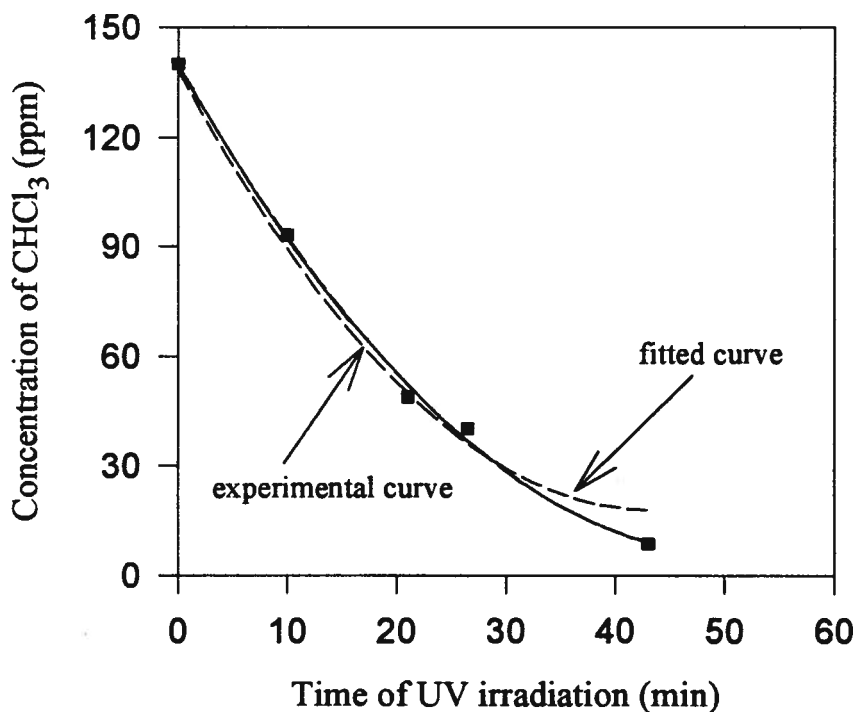

Figure 3.10 The variations of chloroform concentration with UV irradiation time: (—) experimental curve; and (--) fitted curve.

68

According to equation (9), the variations of [Cl^-] with the time used in Figure 3.2 are shown schematically in Figure 3.11. Fitted curve 1 was obtained by using k_2 as the only fitted parameter. k_1 was known as 0.05 min^{-1}, which was calculated from the fitted curve in Figure 3.10. The k_2 value was given as 0.16 min^{-1}. The MSSE value of the fitted curve 1 was 64.96 ppm^2. If k_1 was allowed to vary, the better curve fit (fitted curve 2) with the MSSE value of 36.80 ppm^2 was obtained. The values of k_1 and k_2 were both calculated as 0.08 min^{-1}.
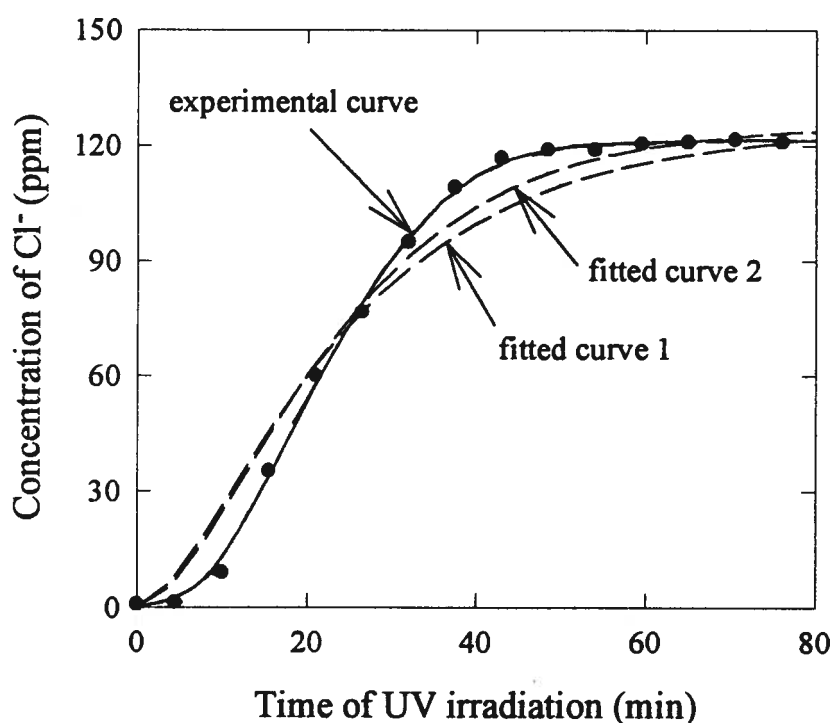

Figure 3.11 Variations of chloride ion concentration with UV irradiation time:

(1) experimental curve, (2) fitted curve 1- k_1 as the only fitted parameter,

and (3) fitted curve 2 - k_1 and k_2 as fitted parameters.

69

The mechanisms of individual step are proposed as follows:

Step 1, adsorption of chloroform molecules on the surface of the TiO$_2$ catalyst. Chloroform molecules in the solution move and reach the surface of TiO$_2$. In the original solution, the concentration of chloroform is much lower than that of water. Chloroform molecules are also less polarized than water molecules. It is believed that the surface of the TiO$_2$ catalyst is mainly covered by water molecules. In addition to the adsorption properties of catalyst and the bonding ability of reactant, the rate of this step mainly depends on the concentration of chloroform and the distance between TiO$_2$ catalysts and chloroform molecules.

The rate of adsorption, R$_S$, can be expected to be proportional to the fraction of coverage (O$_S$) by an adsorbed reactant, S on the illuminated catalyst surface:
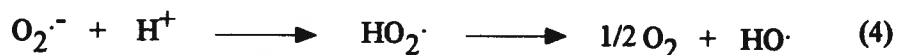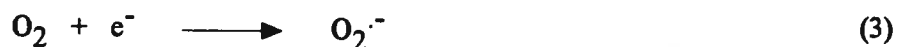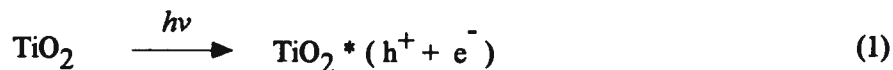
$$R_S = k_1 \, O_S$$

where k$_1$ is the rate constant which is proportional to the available surface area of the catalyst and O$_S$ is given by a Langmuirian isotherm. Thus the rate of adsorption is given by:
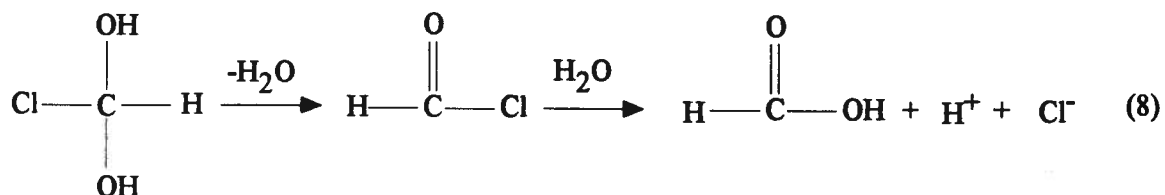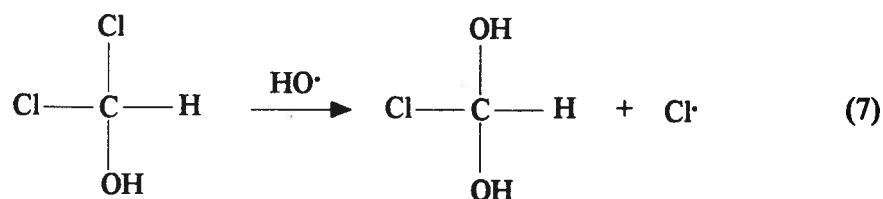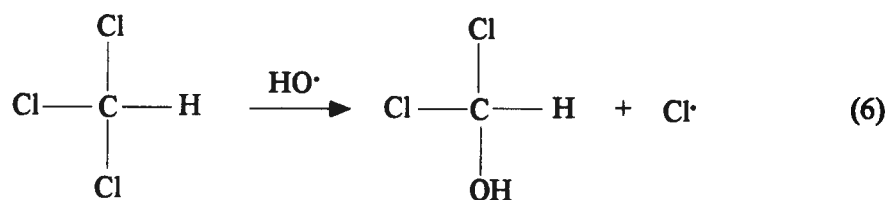
$$R_S = k \, K \, [A] \, / (1 + K \, [A])$$

where K is the adsorption equilibrium constant which is related to the adsorption properties of the catalyst and the bonding ability of the reactant, [A] is the concentration of the reactant.

Step 2, decomposition of chloroform on the surface of the TiO$_2$ catalyst. As noted in Section 1.1.1, under UV irradiation, holes and electrons are created on the TiO$_2$ surface and then HO· radicals are formed. As schematically shown below, hydroxyl radicals would be expected to have the highest concentration on the surface of TiO$_2$. Once a chloroform molecule is absorbed on the surface of TiO$_2$, it will undergo a series of reactions (discussed below) with the hydroxyl radicals to form chloride ions as one final

product. These reactions affect the overall formation rate of chloride ions. The proposed mechanism is as follows:

$$TiO_2 \xrightarrow{h\nu} TiO_2 * (h^+ + e^-) \tag{1}$$

$$H_2O + h^+ \longrightarrow HO\cdot + H^+ \tag{2}$$

$$O_2 + e^- \longrightarrow O_2^{\cdot -} \tag{3}$$

$$O_2^{\cdot -} + H^+ \longrightarrow HO_2\cdot \longrightarrow 1/2\,O_2 + HO\cdot \tag{4}$$

Sub-total reaction (1)+2x(2)+(3)+(4):

$$2H_2O + 2h^+ + e^- + 1/2\,O_2 \longrightarrow 3HO\cdot + H^+ \tag{5}$$

$$\tag{6}$$

$$\tag{7}$$

$$\tag{8}$$

$$\underset{\underset{H}{\overset{O}{\parallel}}}{H-C-OH} \xrightarrow{HO\cdot} HO-\underset{\underset{\parallel}{\overset{O}{\parallel}}}{C}-OH + H\cdot \qquad (9)$$

$$HO-\underset{\overset{O}{\parallel}}{C}-OH \longrightarrow CO_2 + H_2O \qquad (10)$$

$$H\cdot + h^+ \longrightarrow H^+ \qquad (11)$$

$$2Cl\cdot + 2e^- \longrightarrow 2Cl^- \qquad (12)$$
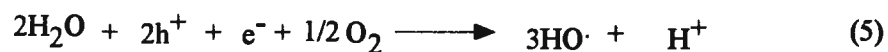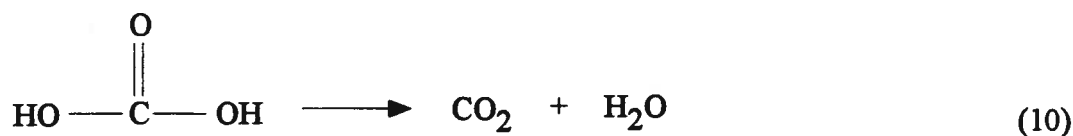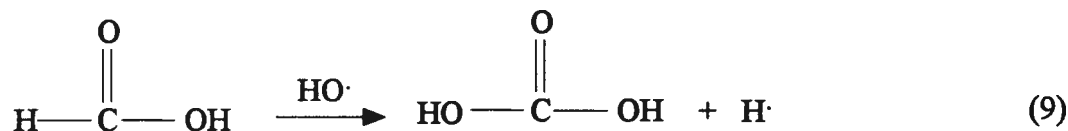
Sub-total reaction (6)+(7)+(8)+(9)+(10)+(11)+(12):

$$CHCl_3 + 3HO\cdot + h^+ + 2e^- \longrightarrow CO_2 + 2H^+ + H_2O + 3Cl^- \qquad (13)$$

Total reaction (5)+(13):

$$CHCl_3 + H_2O + 1/2\,O_2 \longrightarrow CO_2 + 3H^+ + 3Cl^- \qquad (14)$$
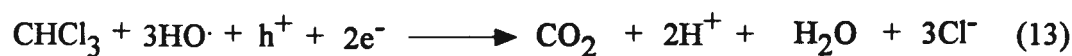
Scheme 3.4 Proposed mechanism of decomposition of chloroform

Step 3, desorption of chloride ions from the surface of TiO₂. Chloride ions formed will desorb from the surface of TiO_2 and diffuse to the bulk solution where they are detected. The catalyst contained in solution was stirred by using a magnetic stirrer during the reaction time and the rate of transfer of Cl^- to bulk solution was dramatically improved. Therefore, the rate of this step was relatively fast and do not affect the overall reaction rate.

72

CHAPTER 4

FURTHER WORK

Development of an in-line automated flow injection analysis (FIA) system for continuous real-time monitoring of photodegradation has been completed. A photo-reactor has been developed which efficiently degrades chloroform in water. The in-line microfilter has provided fast, unpressurized filtration. However, there are still many ways in which the whole system can be improved to increase its efficiency, capability and flexibility. Some advancement strategies and suggestions are detailed below.

4.1   OPTIMIZATION OF THE PHOTOREACTOR

In addition to concentration of titanium dioxide (anatase) in aqueous organic solution, some other important facts should be considered.

pH value

In general, addition of acid into suspended solution can significantly inhibit the rate of reaction. Many compounds show this effect [16, 74]. The photoreactor should be optimized by chosing the best pH value of the degradation for each organic compound.

Oxygen

The oxygen concentration is an important parameter in determining the rate of reaction since oxygen is necessary for the photooxidation [16]. Oxygenated and aerated suspensions should be investigated in the future.

TiO$_2$ glass as catalyst

Glassy TiO$_2$ has shown the potential as a photocatalyst in photodegradation in this study. Increasing its amount and decreasing its size to improve its surface area should be investigated in the future. Its photocatalytical efficiency may exceed that of anatase TiO$_2$ powder while eliminating the separation problem.

4.2   APPLICATION TO MORE COMPOUNDS

The application of this photochemical process should be extended to other chlorinated compounds such as chlorophenols, and even nonchlorinated compounds. Chlorophenols represent an important class of environmental pollutants. They are present in untreated waste water from many pulp and paper mills.

4.3   IMPROVEMENTS TO OPERATING SOFTWARE

The present version of operating software can only obtain data and compute peak quantities such as peak height, peak area from *one* of four ADC channels. The FIA system uses more than one detector in series to obtain different information from more than one channel. For example, a photodetector and chloride ion selective electrode can be used in series to monitor the concentration change of reactant and product. Presently, the information from other present detectors has to be sent to another computer or to a chart recorder. The capability of the FIA system will be greatly improved if the operating software allows more than one ADC channel (more than one detector) to work simultaneously.

4.4   IMPROVEMENTS TO THE FIA MANIFOLD

The present FIA manifold could be improved to monitor the change in concentration of reactant and/or intermediates. Use of a single wavelength flow through photodetector or diode-array spectrophotometry would both be possible. For nonchlorinated compounds such as hydrocarbons, alcohols, *etc.* which give H_2O and CO_2 as final products, a conductivity detector can be used to monitor CO_2 quantitatively. Calibration could use standard CO_2. Detectors can be set in series or in parallel so that one sample injection gives all the information about reactant and product, even any stable intermediates.

To help us identify and characterize the products or intermediates formed, HPLC capability would be added to our present system, as in Figure 4.1. This would be used to monitor degradation of chlorinated or nonchlorinated organics. Two mercury lamps and/or one sonicator horn are immersed in solution. An in-line filter removes the catalyst powder from suspended sample solution. The filtered sample solution is injected by an injection valve into the carrier stream and goes to detectors sequentially. More uninjected sample solution periodically goes into HPLC system via its own injection valve.

The conductivity detector detects the total free ions, or CO_2 itself quantitatively if CO_2 is the only conducting compound in the reaction. The chloride ion selective electrode detects the free chloride ions. The pH electrode monitors the hydrogen ions. The diode array is able to monitor the original organic reactant (at 220 nm in the UV region). It also has the benefits of rapid scanning the solution over the entire UV-vis range, and simultaneous detecting several species at different wavelengths.

In the HPLC system, a sample is injected by the HPLC injection valve into its carrier. It is transported downstream to the column where components in solution are separated and then carried into a UV detector in which the analytes are detected. Stable

intermediates and some products can be separately identified and quantitatively determined.
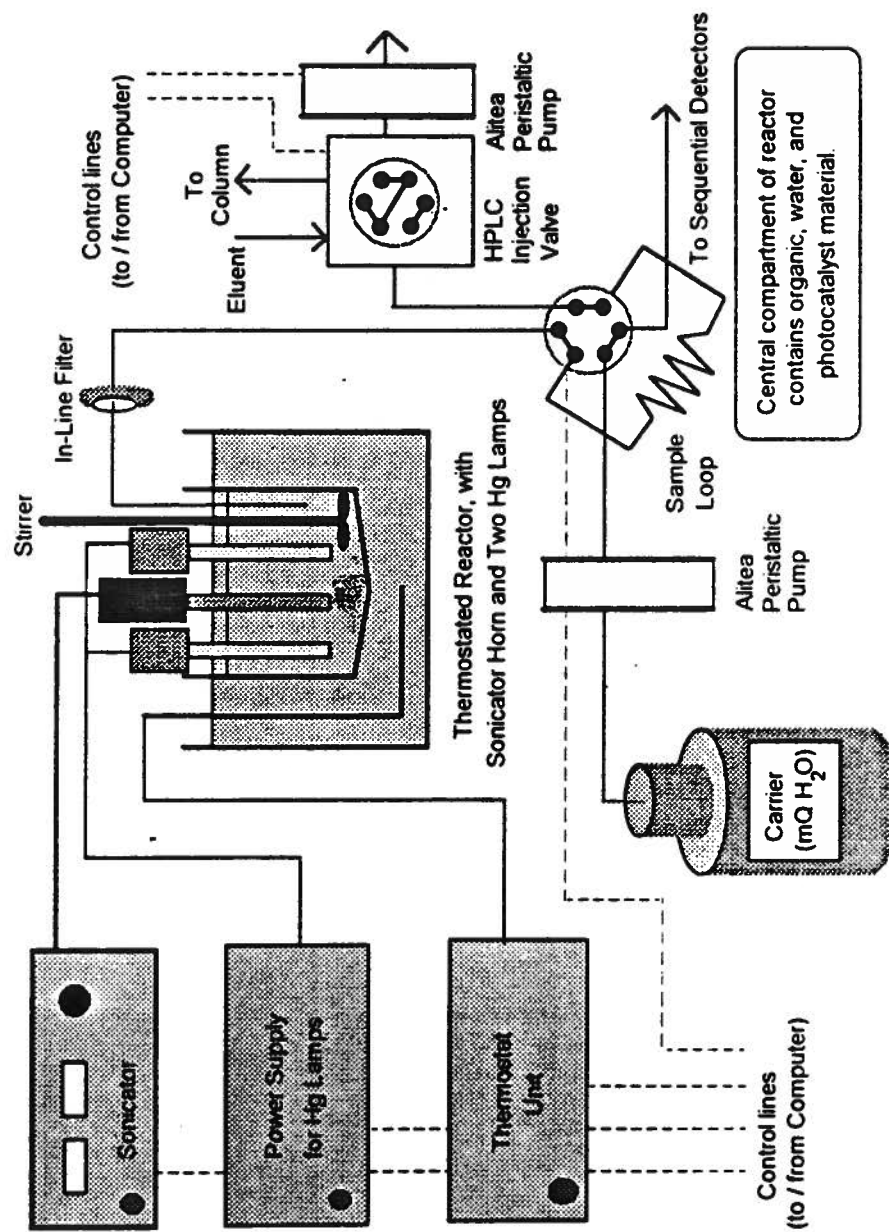
Figure 4.1(a) FIA sampling system with proposed interface to HPLC. Sequential FIA detectors used are: conductivity, Cl⁻-ISE, pH and UV absorbance (spectra).
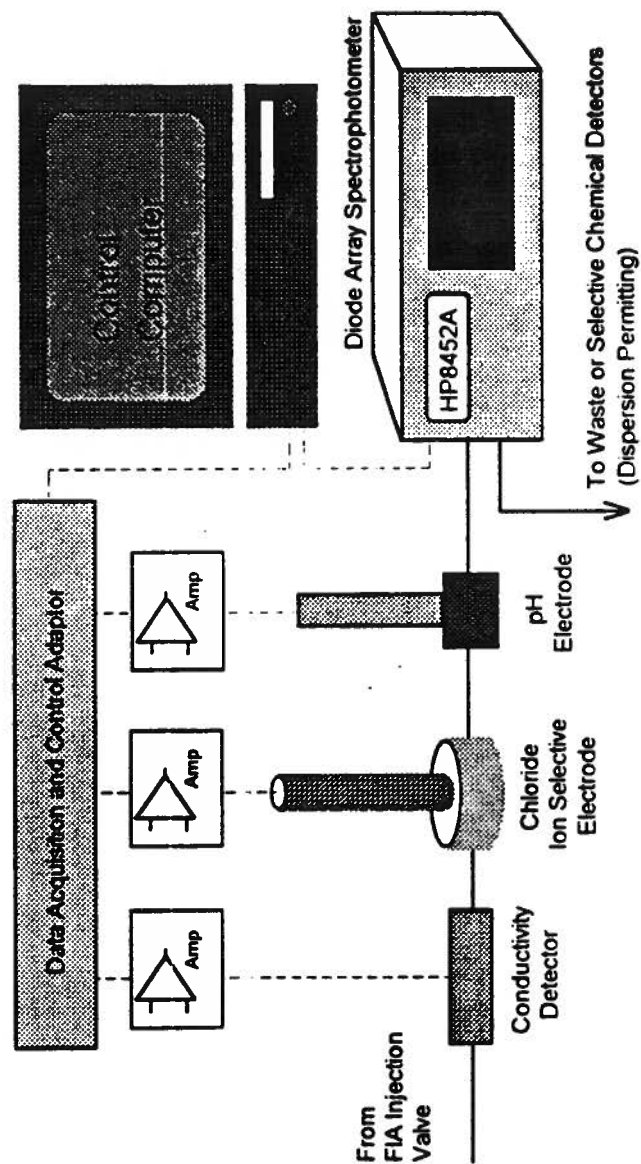
77

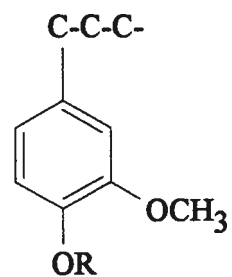**Figure 4.1(b)** Sequential detectors presently available.
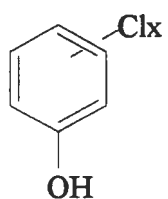
APPENDIX

PRELIMINARY WORK

Chlorinated phenolic compounds have often been singled out as being a particularly toxic group of compounds of industrial origin. Many pulp mills in Canada use chlorine in the bleaching process to remove the brown lignin, a natural product present in all wood pulps. Typically, bleaching is done in 5 or 6 sequential steps, which are designated as chlorination, alkaline extraction, hypoclorite, and chlorine dioxide stage. Effluents are produced by washing the pulp after each stages. During this process, chlorinated phenolics are formed as byproducts by electrophilic aromatic substitution, electrophilic displacement, and dealkylation/demethylation reactions occurring on lignin.

The major phenolics found in pulp and paper effluents can be classified into the following 5 groups of compounds: chlorophenols, chloroguaiacols, chlorocatechols, chlorosyringols and chlorovanillins. The chemical structures of the above compounds are given in Figure A1 [3].
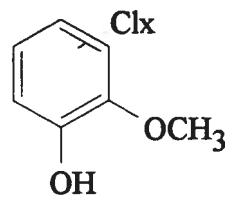
4-chlorophenol was the compound initially studied in this research. Due to the initial unsuccessful development of photo-reactor and filtration system, the reaction was not efficient and the monitoring system was insufficiently precise. Two experiments were carried out: (1) photodegradation of 4-chlorophenol, and (2) chemical degradation of 4-chlorophenol with Fenton's reagent (Fe^{2+} + H_2O_2). In the following sections, we will describe these preliminary experiments, the corresponding results, the reasons that work had been discontinued and the potential to have 4-chlorophenol experiment continued if the new system is used.
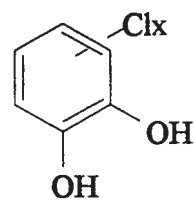
C-C-C-

OCH$_3$

OR

Lignin Unit

Clx

OH

Chlorophenols

Clx

OCH$_3$

OH

Chloroguaiacols

Clx

OH

OH

Chlorocatechols

Clx

CH$_3$O   **OCH$_3$**

OH

Chlorosyringols

CHO

Clx

OCH$_3$

OH

Chlorovanillins

Figure A1 Chemical structures of chlorinated phenolics (from ref. [3])

A.1 EXPERIMENTAL - DECOMPOSITION OF 4-CHLOROPHENOL

All the chemicals used in the experiments were analytical reagent grade quality. All the solutions were prepared using distilled water.

Photodegradation of 4-chlorophenol

The reaction was carried out in a 100 ml glass beaker. An aqueous slurry containing 0.1 wt % titanium dioxide (anatase) and 3.0×10^{-4} M 4-chlorophenol was stirred by a magnetic stirrer. Two UV lamps were located outside of the beaker and the UV irradiation illuminated the solution through the wall of the beaker. Each of 5.00 ml of sample solution was collected at different time of UV irradiation: 5, 10, 20, 30, 40, 50 and 60 minutes. Solutions were filtrated manually through celite layers and made ready for chloride ion determination using a FIA system with chloride ion selective electrode detector (Figure 2.2).

Chemical degradation of 4-chlorophenol with Fenton's reagent $(Fe^{2+} + H_2O_2)$

In this experiment, an 80 ml aqueous solution of 4-chlorophenol and perchloric acid in the selected quantities (10.00 ml of 0.03 M of 4-chlorophenol and 5.00 ml of 0.5 M of $HClO_4$) was thermostated at 23°C and maintained under vigorous stirring. Subsequently, two 5.00 ml aliquots of a $FeSO_4$ (0.01 M) and H_2O_2 (0.5 M) respectively, were added simultaneously to the reaction mixture. The concentration of the chloride ions produced at different reaction times was monitored by an in-line automated FIA system with chloride ion selective electrode (Figure 2.2).

A.2 RESULTS AND DISCUSSION

Photodegradation of 4-chlorophenol

Figure A2 shows the preliminary results for the photodegradation of 4-chlorophenol. The reaction was not efficient. It is evident that there are at least two distinct stages to the detectable reactions. The first occurs within the first 10 minutes of degradation. The second proceeds rapidly after 40 minutes of reaction. There was 47 % chlorine recovered after 60 minutes of reaction.
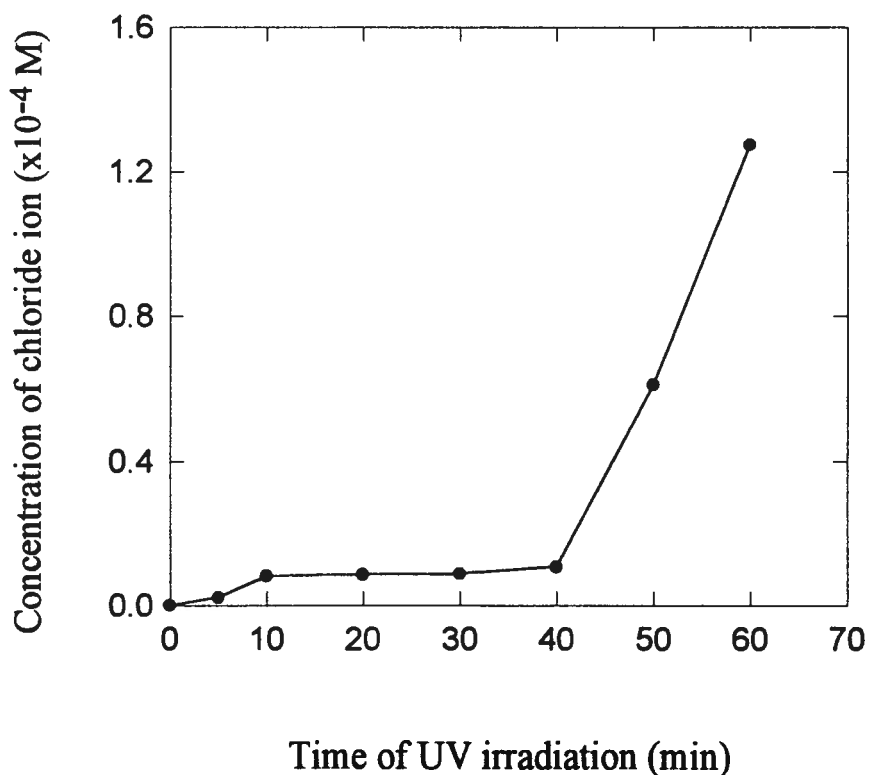

Figure A2 Photodegradation of 4-chlorophenol

The main reasons for discontinuing this work at that time were:

(1)   An effective in-line filtration system to remove catalyst powder had not been found. A celite layer was used to filter out very fine TiO_2 powder manually and it made procedure complicated, tedious, unprecise and inaccurate.

(2)   The photo-reactor had not been fully developed. Two mercury lamps were located outside of the photo-reactor. UV irradiation had been attenuated when it reached the solution because air and the glass of the beaker could absorb UV.

Chemical degradation of 4-chlorophenol with Fenton's reagent ($Fe^{2+} + H_2O_2$)

Photodegradation is based on reaction of organics with hydroxyl radical reaction, Fenton's reagent is another source which generates hydroxyl radicals. To gain insight into the photodegradation reaction without having a complete solution for the above problems, it was decided to make a preliminary study of the chemical degradation of 4-chlorophenol with Fenton's reagent.

Figure A3 depicts the increase in concentration of chloride ion as a function of reaction time. The result demonstrates that the 4-chlorophenol is rapidly degraded in the presence of the Fenton's reagent and an equal (quantitative) amount of free chloride ions in solution was detected.

The presence of Fe^{3+} alone (without any Fe^{2+}) with H_2O_2 had no degrading effect on 4-chlorophenol. The presence of H_2O_2 alone (without any Fe^{2+}) had very little effect.

The results reported may be interpreted on the basis of the following considerations. The interaction of iron (II) ions with hydrogen peroxide yields HO· radicals and iron (III) [38].

$$Fe^{2+} + H_2O_2 \rightarrow Fe^{3+} + HO· + OH^-$$

The HO· formed can easily interact with an aromatic compound inasmuch as HO· radicals are good electrophiles and reactive species. They attack chlorophenol, following which

ring opening occurs to form aldehydes, ketones, acids and the ultimate degradation ensues to CO_2 and HCl (Figure A4) [23].
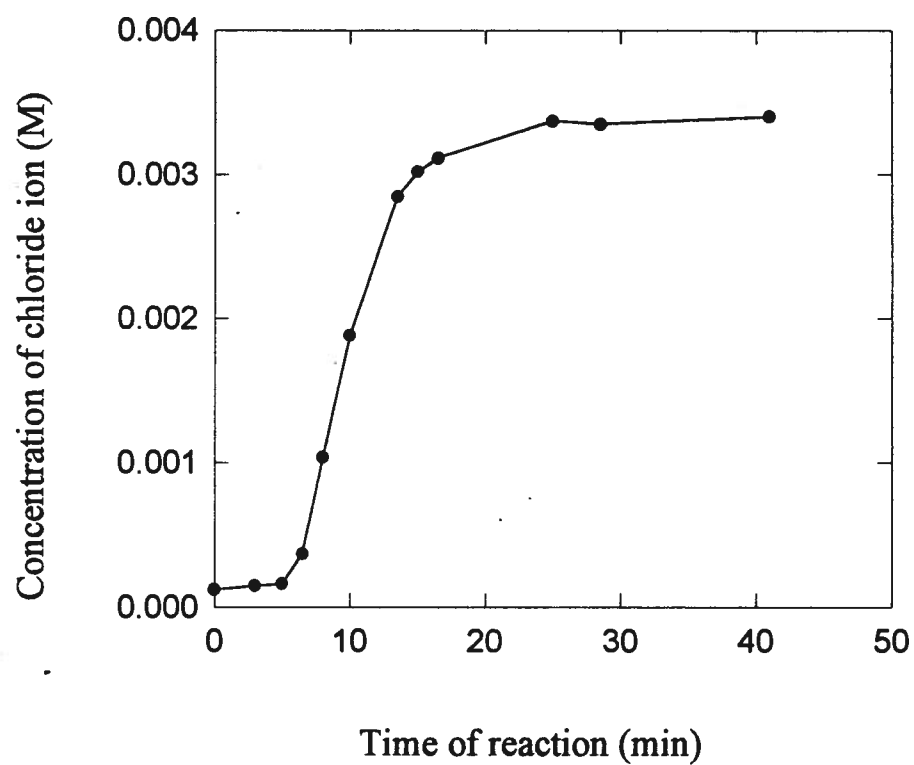

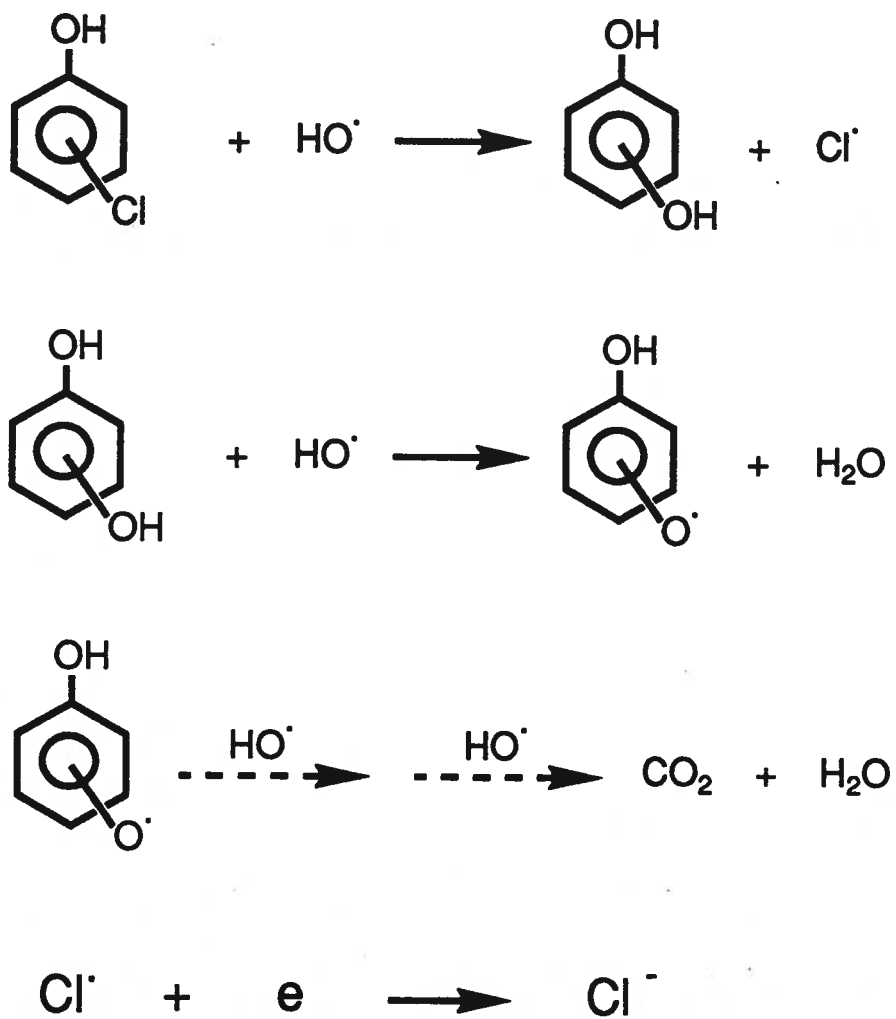**Figure A3** Degradation of 4-chlorophenol with Fenton's reagent

Figure A4 Mechanism of decomposition of chlorophenol (from ref. [23])

To be able to monitor the disappearance of 4-chlorophenol (280 nm) using a spectrophotometric detector, ideally the reactant should be separated from intermediates such as resorcinol before detection. Intermediates interfered with the spectrophotometric detection of reactant since their absorption peaks overlapped with these of the reactant (Figure. A5). Therefore, use of an HPLC technique equipped with a spectrophotometric detector would be best suitable for this purpose. The calibration curve of 4-chlorophenol whose absorbance was detected at 280 nm is shown in Figure. A6.

Power ultrasound provided little effect to this reaction since amount of HO· radicals generated from water by ultrasound is ignorable compared to the amount of HO· produced from Fenton's reagent.
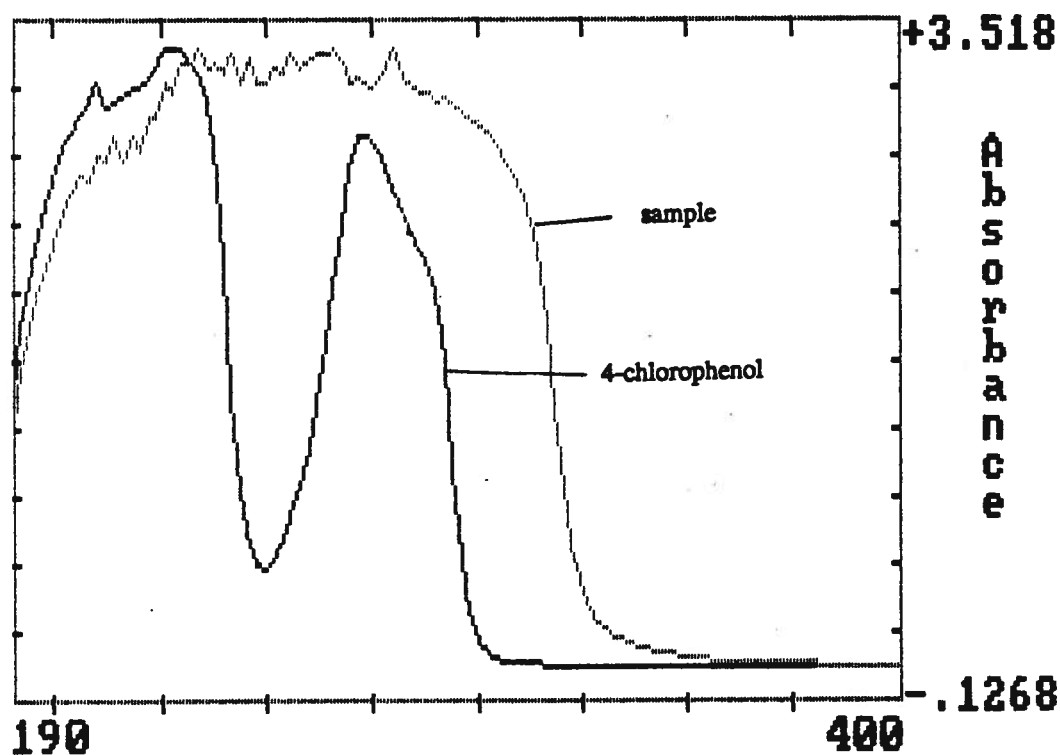

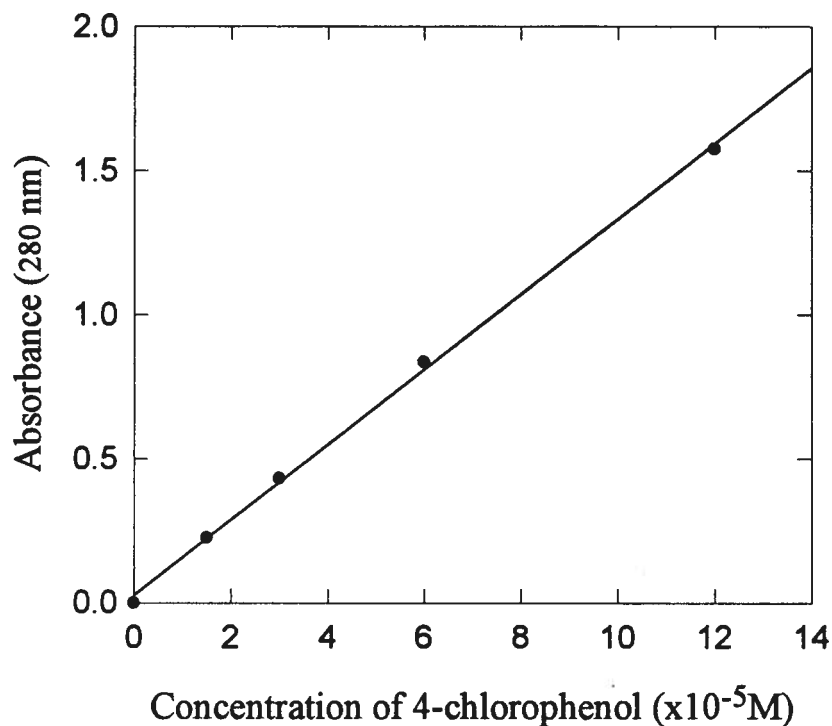Figure A5 UV spectra of 4-chlorophenol and a photodegaded sample

Figure A6 Calibration curve of 4-chlorophenol

(The calculated molar absorptivity coefficient: $\varepsilon_{calculated} = 13352 \, l \, cm^{-1}mol^{-1}$)

A.3   POTENTIAL TO CONTINUE THE STUDY OF 4-CHLOROPHENOL WITH NEW DEGRADATION AND MONITORING SYSTEM

With the degradation and monitoring system we successfully developed (Figure 2.1 and Figure 2.2), 4-chlorophenol should be photodegraded efficiently and the process could be easily monitored in-line. The new system has eliminated the catalyst separation problem by inserting a micro-filter in the sampling line and an efficient photo-reactor was obtained by directly immersing UV lamps in the sample solution. Generally, most chlorinated compounds are compatible with the system as developed.

REFERENCES

(1) State of the Environment Bulletin, No. 93-1, State of the Environment Reporting, Environment Canada, Ottawa, Ontario.

(2) B. Fleming, Pulp & Paper, 4, (1991) 115.

(3) H. Lee, R. L. Hong-You and P. J. A. Fowlie, J. Assoc. Off. Anal. Chem., 72(6), (1989) 979.

(4) J. J. Rook, Water Treat. Exam., 23, (1974) 234.

(5) S. W. Krasner, Research and Technology, August, (1989) 41.

(6) T. A. Bellar, J. J. Lichtenberg and R. D. Kroner, J. Am. Water Works Assoc. 66, (1974) 703.

(7) B. G. Oliver, and J. Lawrence, J. Am. Water Works Assoc. 71, (1979) 161.

(8) S. Kaye, "Handbook of Emergency Toxicology", 4th edition, Charles C. Thomas Publisher, Illinois, USA, 1980.

(9) M. P. Streir, Environ. Sci. Technol, 14, (1980) 28.

(10) R. W. Matthews, Sunworld, 9(1), (1985) 3.

(11) E. R. Hall, J. Fraser, S. Garden and L-A. Cornacchio, Pulp & Paper Canada, 90(11), (1989) 68.

(12) R. J. Caron and D. W. Reeve, "1991 Pulp and Paper Industry Environment Conference", Quebec, October, 1991.

(13) R. J. Crowford, M. N. Stryker, S. W. Jett, W. L. Carpenter, R. P. Fisher and A. K. Jain, Tappi Journal, November, (1987) 123.

(14) A. L. Pruden and D. F. Ollis, J. Catal., 82, (1983) 404.

(15) H. H. Cheng, "Pesticides in the Soil Environment: Processes, Impacts, and Modeling", Madison, Wis., USA, p174, 1990.

(16) C. Hsiao, C. Lee and D. F. Ollis, J. Catal. 82, (1983) 418.

(17) R. W. Matthews, Aust. J. Chem., 40 (1987) 667.

(18)   A. L. Pruden and D. Ollis, Environ. Sci. Technol., 17, (1983) 628.

(19)   D F. Ollis, Environ. Sci. Technol., 19, (1985) 481.

(20)   M. Barbeni, E. Pramauro, E. Pelizzetti, E. Borgarello M. Gratzel and N. Serpone, Nouv. J. Chim., 8, (1984) 547.

(21)   M. Barbeni, E. Pramauro, E. Pelizzetti, E. Borgarello and N. Serpone, Chemosphere, 14 (2), (1985) 195.

(22)   R. W. Matthews, J. Phys. Chem., 91, (1987) 3328.

(23)   I. Izumi, W. W. Dunn, K. O. Wilbourn, F. F. Fan and A.J.Bard, J. Phys. Chem., 84 (1980) 3207.

(24)   Y. Shimamura, H. Misawa,.T. Oguchi, T. Kanno, H. Sakuragi and K. Tokumaru, Chem. Lett., (1983)   1691.

(25)   C. D. Jaeger and A. J. Bard, J. Phys. Chem., 83, (1979) 3146.

(26)   I. Izumi, F. Fan and A. J. Bard, J. Phys. Chem., 85, (1981) 218.

(27)   M. Barbeni, C. Minero, and E. Pelizzettei, Chemosphere 16, (1988) 1987.

(28)   B. Kraeutler and A.J. Bard, J. Am. Chem. Soc., 100 (1978) 5985.

(29)   B. Kraeutler and A.J. Bard, J. Am. Chem. Soc., 100 (1978) 2239.

(30)   L. L. Turai and F. D. Rosario, Applita, 35, (1982) 407.

(31)   D. Bremner, Chemistry in Britain, July, (1986) 633.

(32)   T. J. Mason, Canadian Chemical News, March, (1991) 25.

(33)   K. S. Suslick and D. J. Casadonte, J. Am. Chem. Soc., 109, (1987) 3459.

(34)   K. S. Suslick, Scientific American, February, (1989) 80.

(35)   L. L Turai, C. M. Parkinson, S. G. Hornor and M. J. Mitchell, Tappi, 63, (1980) 81.

(36)   T. J. Mason and J. P. Lorimer, "Sonochemistry", Wiley, 1988.

(37)   K. S. Suslick, D. A. Hammerton and R. E. Cline, J. Am. Chem. Soc., 108, (1986) 5641.

(38) (a) M. Barbeni, C. Minero, E. Pelizzetti, E. Borgarello and N. Serpone, Chemosphere, 16, (1988) 2225.

(b) C. K. Gratzel, M. Jirousek and M. Gratzel, J. Mol. Catal., 39 (1987) 347.

(39) J. V. Dust and W. S. Thomson, For. Prod. J., 23 (9), (1973) 59.

(40) E. J. Kirsch and J. E. Etzel, J. Wat. Pollut. Control Fed., 45, (1973) 359.

(41) D. W. Ferguson, J. T. Gramith and M. J. McGuire, J. Am. Water Works Assoc. May 1991.

(42) E. M. Aieta, J. Am. Water Works Assoc. May 1988.

(43) C. Johnston, Pulp and Paper, 65(11), (1991) 23.

(44) N.Takahashi, "Ozonation of Several Organic Compounds Having Low Molecular Weight Under Ultraviolet Irradiation.", Ozone Sci. & Engineering, 12:1:1(1990).

(45) J. J. Santoleri, Chem. Eng. Prog. 69, (1973) 68.

(46) J. Ruzicka and E. H. Hansen, "Flow Injection Analysis", Wiley, New York (1988).

(47) J. Ruzicka and E. H. Hansen, Anal. Chim. Acta, 78 (1975)145.

(48) C. G. Enke and T. A. Nieman, Anal. Chem., 48 (1976), 705A.

(49) C. S. Willliams, Designing Digital Filters, Prentice-Hall: Englewood Cliffs, 1986, p. 2.

(50) L. J. Wachel in D. P. Manka (Ed.), Automated Stream Analysis for Process Control, Academic Press, New York, 1984, Vol. 2, Chap.15.

(51) W. E. Van der Linden, Anal. Chim. Acta, 179, (1986) 91.

(52) D. K. Wolcott and D. G. Hunt, Paper presented at the 11th Annual Meeting of the Federation of Analytical Chemistry and Spectroscopy Societies, Philadelphia, 1984.

(53) R. A. Mowery Jr., Instrum. Technol., May, (1984) 51.

(54) R. A. Mowery Jr., ISA Trans., 24, (1985) 1.

(55) C. C. Lee and B. D. Pollard, Anal. Chim. Acta, 158, (1984) 157.

(56) A. Schelter-Graf, H. L. Schmidt, and H. Huck, Anal. Chim. Acta, 163, (1984) 299.

(57)   B. Bernhardsson, E. Martins, and G. Johansson, Anal. Chim. Acta, 167, (1985) 111.

(58)   M. J. Whitaker, Laboratory Note: *Industrial Applications of FIA*, Amer. Lab., 18(3), (1986) 154.

(59)   J. Ruzicka, Chemtech, 17, (1987) 96.

(60)   T. Korenage and H. Ikatsu, Bunseki Kagaku, 31, (1982) 135 (in Japanese).

(61)   C . F. Mandenius, B. Danielsson, and B. Mattiasson, Anal. Chim. Acta, 163, (1984) 135.

(62)   S. Chung, X. Wen, K. Vilholm, M. D. Bang, G. Christian and J. Ruzicka, Anal. Chim. Acta, 249, (1991) 77.

(63)   L. W. Forman, B. D. Thomas and F. S. Jacobson, Anal. Chim. Acta, 249, (1991) 101.

(64)   M. Nilsson, H. Hakanson and B. Mattiasson, Anal. Chim. Acta, 249, (1991) 163.

(65)   K. Schugerl, L. Brandes, T. Dullau, K. Holzhauer-Rieger, S. Hotop, U. Hubner, X. Wu and W. Zhou, Anal. Chim. Acta, 248, (1991) 87.

(66)   J. Ruzicka, Anal. Chim. Acta, 190, (1986) 155.

(67)   M. Gisin and C. Thommen, Anal. Chim. Acta, 190, (1986) 165.

(68)   A. J. Bard, J. Photochem., 10, (1979) 59.

(69)   M. A. Fox, Chemtech, 22(11), (1992) 680.

(70)   R. W. Matthews, J. Catal., 111, (1988) 264.

(71)   S. Tunesi, and M. A. Anderson, Chemosphere, 26(7), (1987) 1447.

(72)   G. K-C. Low, S. R. McEvoy, and R. W. Matthews, Environ. Sci. Technol., 104, (1991) 71.

(73)   W. A. Zeltner, C. G. Hill and J. M. Anderson, Chemtech, 23(5), (1993) 21.

(74)   G. K.-C. Low and R. W. Matthews, Anal. Chim. Acta, 231, (1990) 13.

(75) P. D. Wentzell, A. P. Wade, P. M. Shiundu, R. M. Ree, M. Hatton, T. J. Sly and
      D. Betteridge, J. Automatic Chem., 11(5), (1989) 227.

(76) A. P. Wade, P. M. Shiundu and P. D. Wentzell, Anal. Chim. Acta, 237, (1990)
      361.

(77) P. M. Shiundu and A. P. Wade, J. Automatic Chem., 13, (1991) 83.

(78) H. Tominaga, S. Tanaka and N. Tomina, Nephron, 42, (1986) 128

(79) L. Kruczynski, H. D. Gesser, C. W. Turner and E. A. Seers, Nature, 291, (1981)
      399.

(80) H. D. Gesser, L. Krucczynski and Y. S. Yong, J. Colloid Interface Sci., 135,
      (1990) 1.

(81) A. Henglein and Ch.-H. Fisher, Ber. Bunsenges, Phys. Chem., 88, (1984) 1196.

(82) T. J. Mason, "Chemistry With Ultrasound", Society of Chemical Industry (SCI),
      London and New York, (1990), p105.